

# Technical Note: Comparison of radiometric techniques for estimating recent organic carbon sequestration rates in ~~freshwater mineral soil wetlands~~ temperate inland wetland soils

Purbasha Mistry<sup>1</sup>, Irena F. Creed<sup>1,2</sup>, Charles G. Trick<sup>3</sup>, Eric Enanga<sup>2</sup>, David A. Lobb<sup>4</sup>

<sup>1</sup> School of Environment and Sustainability, University of Saskatchewan, 117 Science Place, Saskatoon, SK, S7N 5C8, Canada

<sup>2</sup> Department of Physical and Environmental Sciences, University of Toronto, 1265 Military Trail, Toronto, ON, M1C 1A4, Canada

<sup>3</sup> Department of Health and Society, University of Toronto, 1265 Military Trail, Toronto, ON, M1C 1A4, Canada

<sup>4</sup> Department of Soil Science, University of Manitoba, 13 Freedman Crescent, Winnipeg, MB, R3T 2N2, Canada

Correspondence to: Irena F. Creed (irena.creed@utoronto.ca)

**Abstract.** For wetlands to serve as natural climate solutions, accurate estimates of organic carbon (OC) sequestration rates in wetland sediments are needed. Dating using cesium-137 (<sup>137</sup>Cs) and lead-210 (<sup>210</sup>Pb) radioisotopes is commonly used for measuring OC sequestration rates in wetland sediments. <sup>137</sup>Cs radioisotope dating is relatively simple, with calculations based on a single point representing the onset (1954) or peak (1963) of the <sup>137</sup>Cs fallout. <sup>210</sup>Pb radioisotope dating is more complex as the calculations are based on multiple points. Here, we show that reliable dating of sediment cores collected from wetlands can be achieved using either <sup>137</sup>Cs or <sup>210</sup>Pb dating, or their combination. However, <sup>137</sup>Cs and <sup>210</sup>Pb profiles along the depth of sediment cores need to be screened, analyzed, and interpreted carefully to estimate OC sequestration rates with high precision. To this end, we propose a decision framework for screening <sup>137</sup>Cs and <sup>210</sup>Pb profiles into high- and low-quality sediment profiles, and we compare dating using the 1954 and 1963 time-markers, i.e., the rates of sedimentation and, consequently, OC sequestration over the past ~60 years. Our findings suggest that <sup>137</sup>Cs- and <sup>210</sup>Pb-based OC sequestration rates are comparable, especially when using the 1963 (vs. 1954) time-marker.

## 1 Introduction

Wetlands in agricultural landscapes serve a crucial role in providing habitat for wildlife, regulating climate, improving water quality, and ~~preventing~~ reducing floods. Moreover, these wetlands have the potential to sequester organic carbon (OC), ~~making them~~ (Bridgham et al., 2006; Nahlik and Fennessey, 2016; Bansal et al., 2023). Accounting for the balance between the sequestration and emission of carbon can help establish wetlands as essential candidates ~~to be~~ for natural climate solutions by offsetting carbon emissions (Hambäck et al., 2023). These wetlands embedded in agricultural landscapes are recognized as temperate inland wetland soils. The global carbon stock of temperate inland wetland soils is estimated to be 46 Pg C to 2

29 m depth, and Canada's temperate inland wetland soils are estimated to contain 4.6 Pg C (Bridgham et al., 2006). Compared  
30 to peatlands, the rapid rate of OC sequestration and the more considerable spatial extent of temperate inland wetland soils  
31 can help contribute significantly to regional or national carbon sequestration (Bridgham et al., 2006; Nahlik and Fennessey,  
32 2016).

33  
34 Canada encompasses around 25% of the world's wetlands, with an area of approximately 1.29 million square kilometers,  
35 which accounts for 13% of the country's terrestrial area (Environment and Climate Change Canada, 2016), highlighting the  
36 global importance of these wetlands. Unfortunately, there is minimal data on the OC sequestration rates in these wetlands.  
37 To estimate the OC sequestration potential of these wetlands, it is ~~critical~~ essential to establish precise measurements to  
38 quantify wetland OC sequestration, develop strategies to promote conservation and restoration efforts, incorporate carbon  
39 credits in the carbon markets, and validate the wetland-based ecosystem services.

40  
41 There are several ways to estimate the potential of wetlands to store OC (Bansal et al., 2023). One of these methods is  
42 radiometric dating, which can ~~estimate~~ calculate the OC storage rates of wetlands over periods of 10 to  $\geq 1,000$  years.  
43 Frequently used radioisotopes for radiometric dating are cesium-137 ( $^{137}\text{Cs}$ ) and lead-210 ( $^{210}\text{Pb}$ ), which can be used to  
44 estimate relatively recent (up to the last 100 years) OC sequestration rates (Villa and Bernal, 2018). ~~The estimation~~  
45 ~~of~~ Estimating OC sequestration rates involves building an age-depth profile or model of  $^{137}\text{Cs}$  and  $^{210}\text{Pb}$  from sediment cores  
46 that demonstrate the relationship between the depth of sediment layers and their corresponding age. Since the inorganic  
47 radioisotopes ( $^{137}\text{Cs}$  and  $^{210}\text{Pb}$ ) strongly bind with the soil particles once in contact, the radioisotopes can act as an efficient  
48 tracer for investigating OC sequestration rates (Ritchie and McHenry, 1990; Craft and Casey, 2000). These characteristics  
49 allow for accurate tracking of carbon movement within ecosystems, thereby enabling the extraction of detailed information  
50 about carbon sequestration dynamics in wetlands.

51  
52 The characteristics of  $^{137}\text{Cs}$  and  $^{210}\text{Pb}$  to estimate wetland OC sequestration rates are presented in Table 1.  $^{137}\text{Cs}$  is an  
53 artificial radioisotope ~~which~~ that was ~~formed due to~~ produced during thermonuclear bomb testing in the 1950s and 1960s,  
54 with the onset of atmospheric deposition in 1954 and a peak in 1963 (Ritchie and McHenry, 1990). The testing caused  
55 radioactive uranium to decay, and, as a result,  $^{137}\text{Cs}$  isotope was released into the atmosphere, which was then deposited  
56 around the globe. ~~Although there may be challenges in applying our study to some parts of the world, the information is~~  
57 ~~generally applicable and valuable for consideration in all regions. We encourage others to customize this approach further~~  
58 ~~for use in other regions where Cs deposition histories vary.~~

59

60  $^{137}\text{Cs}$  has a half-life of 30.17 years, which can be used to estimate the last ~50-70 years of OC sequestration rates in wetlands  
61 (e.g., Bernal and Mitsch, 2012).  $^{137}\text{Cs}$  dating assumes constant sedimentation rates measured since 1954 ~~and 1963~~ or 1963.  
62 In using the two time-markers for  $^{137}\text{Cs}$ , we do not expect the sedimentation rates to be equal, but we do expect them to be  
63 similar. The onset and the peak of  $^{137}\text{Cs}$  activity at 661.6 keV can be used to mark 1954 and 1963, respectively. These time-  
64 markers (1954 and 1963) can ~~be used to~~ date sediment layers (Pennington et al., 1973; Ritchie and McHenry, 1990; DeLaune  
65 et al., 2003) and consequently the OC sequestration rates.  $^{137}\text{Cs}$  has an additional time-marker for Europe in 1986 due to the  
66 Chernobyl nuclear accident and for Japan in 2011 due to the Fukushima Daiichi nuclear accident (Foucher et al., 2021),  
67 indicating that OC sequestration estimates can be derived for different timescales. In the Americas, we do not see evidence  
68 of the 1986 or 2011  $^{137}\text{Cs}$  peak, which is observed in Europe and Japan, respectively, so we did not need to use other  
69 radioisotope techniques (e.g.,  $^{239+240}\text{Pu}$ ) to distinguish the 1986 or 2011  $^{137}\text{Cs}$  peak from the 1963  $^{137}\text{Cs}$  peak.  $^{137}\text{Cs}$  dating  
70 requires a gamma spectrometer to estimate OC sequestration rates. Sample preparation for gamma analysis involves drying,  
71 weighing, disaggregating, homogenizing, and sieving (Bansal et al., 2023). Samples vary from 1 to 1,500 g, with smaller  
72 samples associated with higher uncertainties and, therefore, requiring longer times to analyze. Gamma analysis counting  
73 times range from 4 to 48 h for each sample (e.g., 4 to 12 h in Li et al., 2007; 12 to 24 h in Zarrinabadi et al., 2023, ~~and 24 to~~  
74 ~~48 h in Kamula et al., 2017~~).  ~~$^{137}\text{C}$  dating calculations are less complicated than  $^{210}\text{Pb}$ , with little modelling knowledge or~~  
75 ~~expertise needed (Breithaupt et al., 2018)~~; and 24 to 48 h in Kamula et al., 2017).  $^{137}\text{Cs}$  dating provides a simple result (an  
76 average sedimentation rate), while  $^{210}\text{Pb}$  dating provides a more complex result (using a supply rate model to reveal trends in  
77 sedimentation rates). Plutonium (Pu) may replace  $^{137}\text{Cs}$  in the future due to concerns of half-life and persistence as a dating  
78 tool. In essence,  $^{239+240}\text{Pu}$  has the same source and deposition mechanism as  $^{137}\text{Cs}$ . Its longer half-life will make its peak  
79 measurable when  $^{137}\text{Cs}$  is no longer measurable.

80  
81 Unlike  $^{137}\text{Cs}$ ,  $^{210}\text{Pb}$  is a naturally occurring radionuclide ~~of~~ derived from  $^{238}\text{U}$  and deposits atmospherically from the decay of  
82 radium-226 ( $^{226}\text{Ra}$ ) (Walling and He, 1999).  $^{210}\text{Pb}$  has a half-life of 22.3- years and is used to estimate the last 10-150 years  
83 of OC sequestration rates in wetlands (Craft and Richardson, 1998; Craft and Casey, 2000; Craft et al., 2018; Creed et al.,  
84 2022).  $^{210}\text{Pb}$  activity can be measured using gamma (observed at 46.5 keV) and alpha spectrometry (destructive) (Walling  
85 and He, 1999; Bellucci et al., 2007). Traditional alpha analysis requires 0.2-0.5 g of sample and additional sample  
86 preparation involving leaching with hydrochloric and nitric acid and electroplating (up to 24 h for sample preparation)  
87 (Bansal et al., 2023). Alpha analysis can be considered an indirect method for  $^{210}\text{Pb}$  dating where polonium-210 ( $^{210}\text{Po}$ )  
88 activity is measured, assuming both  $^{210}\text{Pb}$  and  $^{210}\text{Po}$  are in a secular equilibrium.  $^{210}\text{Pb}$  activity is calculated by comparing  
89  $^{210}\text{Po}$  activity against the known activity of  $^{209}\text{Po}$  (isotope tracer). In alpha analysis, the additional time required for sample  
90 preparation is compensated ~~for~~ by running multiple samples simultaneously (Bansal et al., 2023). Gamma and alpha  
91 spectrometry of  $^{210}\text{Pb}$  provides the total  $^{210}\text{Pb}$  activity, which incorporates unsupported (or excess)  $^{210}\text{Pb}$  ( $^{210}\text{Pb}_{\text{ex}}$ ) and

92 supported  $^{210}\text{Pb}$ .  $^{210}\text{Pb}_{\text{ex}}$  is used to determine the ~~sediment accumulation rate~~-mass or sediment accumulation rate. Supported  
93  $^{210}\text{Pb}$  is derived from the natural decay of  $^{226}\text{Ra}$  in the sediment, while unsupported  $^{210}\text{Pb}$  comes from the decay of  
94 atmospheric radon-222 ( $^{222}\text{Rn}$ ), which deposits  $^{210}\text{Pb}$  onto the sediment surface from the air. Unsupported  $^{210}\text{Pb}$  activity  
95 decreases over time due to radioactive decay, unlike supported  $^{210}\text{Pb}$  (Appleby and Oldfield, 1983). The choice of model  
96 used in  $^{210}\text{Pb}$  dating can reflect constant and variable sedimentation rates (Sanchez-Cabeza and Ruiz-Fernandez, 2012) and,  
97 consequently, OC sequestration rates in wetlands. Some models used for  $^{210}\text{Pb}$  dating are (1) constant flux-constant  
98 sedimentation (CFCS) model, (2) constant rate of supply (CRS) model, and (3) constant initial concentration (CIC) model  
99 (Appleby and Oldfield, 1978; ~~Sanchez Cabeza and Ruiz Fernandez, 2012; Kamula et al., 2017~~). Both  $^{137}\text{Cs}$  and  $^{210}\text{Pb}$   
100 provide suitable time-markers and a longer time horizon compared to direct measurements using the time-marker of horizons  
101 (2-10 years) to study sediment accretion and, subsequently, OC sequestration rates in wetlands (Bernal and Mitsch, 2013;  
102 Villa and Bernal, 2018). In this study, we compared the average OC sequestration rate derived from  $^{137}\text{Cs}$  temporal markers  
103 with the progressive OC sequestration rates derived using a constant rate of supply model applied to  $^{210}\text{Pb}$ .

**Table 1: Characteristics of  $^{137}\text{Cs}$  and unsupported  $^{210}\text{Pb}$  ( $^{210}\text{Pb}_{\text{ex}}$ ) dating to estimate sedimentation rates in wetlands.**

Method of radiometric dating	$^{137}\text{Cs}$	$^{210}\text{Pb}_{\text{ex}}$
Type of radioisotope	Artificial (atmospheric deposition 1954 – 1963).	Natural.
Half life	30.17 years.	22.3 years.
Time-marker	1954 (onset) and 1963 (peak).	Recent (10-20 years) to a maximum of 50-150 years.
Radiometric Technique	Gamma spectrometry (nondestructive).	Gamma (nondestructive) and alpha spectrometry (destructive).
Pre-processing	Drying, weighing, disaggregating, homogenizing, and sieving.	For gamma analysis, drying, weighing, disaggregating, homogenizing, and sieving prior to analysis on a gamma counter.  For alpha analysis, leaching with hydrochloric and nitric acid and electroplating of $^{210}\text{Po}$ which constitutes allowing the digested and therefore extracted $^{210}\text{Po}$ isotope solution to settle on silver coins overnight before measuring the $^{210}\text{Po}$ (known tracer) and $^{210}\text{Po}$ activity (sample) next morning through the alpha counter/ensemble.
Sample size	Minimum 1 g (larger sample size has higher certainty).	1 to 5 g for gamma spectrometry, 0.2 to 0.5 g for alpha spectrometry.
Time requirement for radiometric dating	48 h for each sample for gamma spectrometry.	48 h for each sample for gamma spectrometry. 48 to 72 h for multiple samples plus sample preparation time per multiple samples.
Output	A single average sedimentation rate.	Variable sedimentation rate.
Estimation approach	Onset of $^{137}\text{Cs}$ activity represents 1954 and highest peak of $^{137}\text{Cs}$ activity represents 1963, observed at 661.6 keV.	Activity of $^{210}\text{Pb}$ is observed at 46.5 keV. Excess $^{210}\text{Pb}$ is used to determine the vertical accretion.
Complexity in estimation	Simple; estimated by using time-marker of onset or peak $^{137}\text{Cs}$ activity and associated <b>sedimentation</b> sediment accumulation.	More complex; estimated by one of several models to estimate sedimentation rate. Most common models are (1) constant flux–constant sedimentation model, (2) constant rate of supply model, and (3) constant initial concentration model (Appleby and Oldfield, 1978; <b>Sanchez-Cabeza and Ruiz-Fernandez; Kamula et al., 2017</b> )

105

106 The combined use of  $^{137}\text{Cs}$  and  $^{210}\text{Pb}$  may improve the accuracy of the dating estimation, ~~according to~~ (Drexler et al. (, 2018) and; Creed et al. (, 2022). The more detailed assessment accrues a higher cost and time requirement, and the need for  
107 specialized equipment and technical expertise to conduct laboratory and data analyses may constrain the research efforts  
108 (Bansal et al., 2023). Furthermore, factors such as timescales, analytical complexity in interpreting radioisotope profiles  
109 (e.g.,  $^{137}\text{Cs}$  peak clarity), variability in atmospheric deposition, and mobilization of radioisotopes can contribute to  
110 uncertainty (Drexler et al., 2018; Loder and Finkelstein, 2020; Zhang et al., 2021; Bansal et al., 2023) and limit the  
111

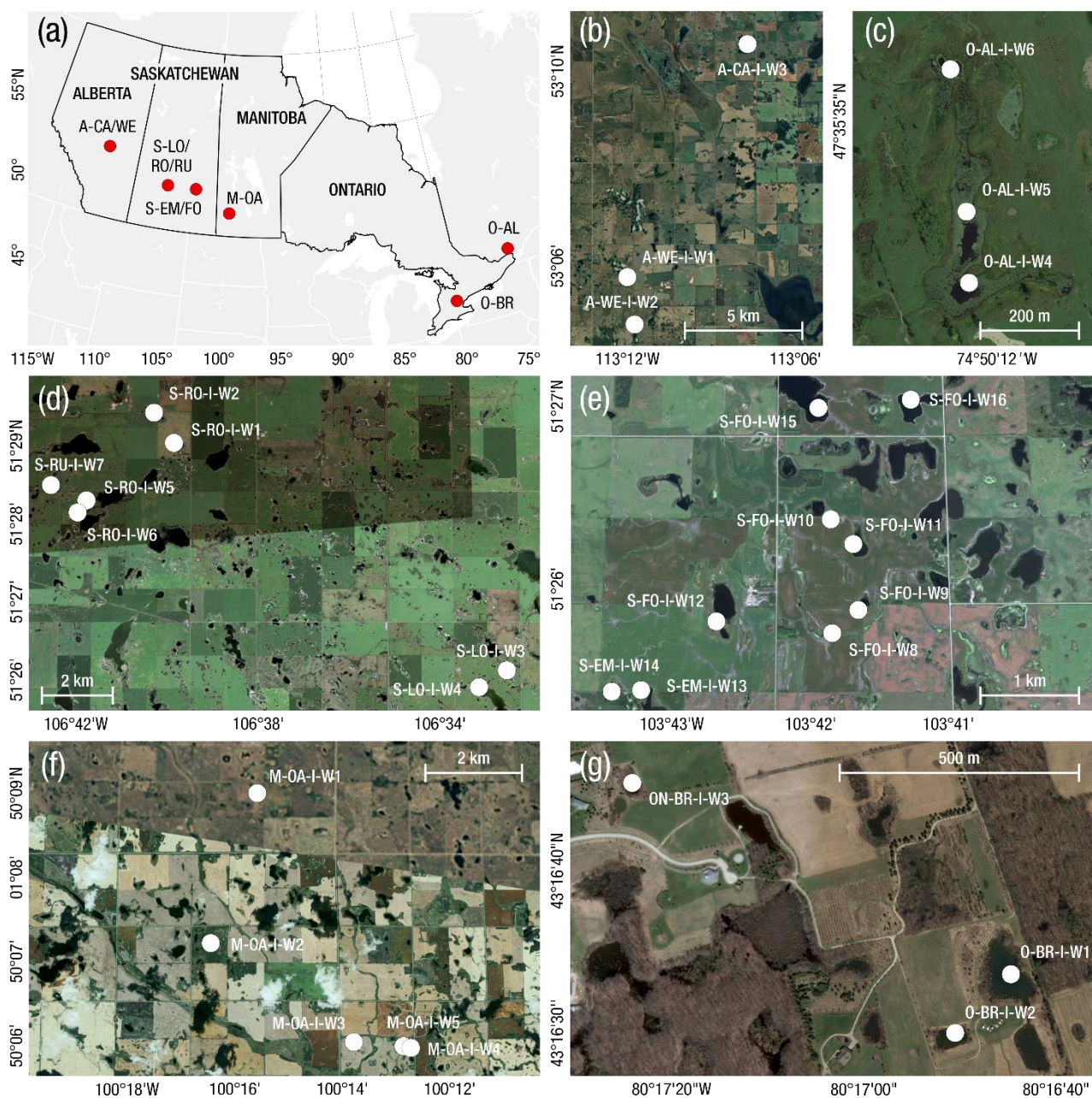
112 applicability of one radioisotope over the other. Therefore, it is essential to consider the advantages and potential challenges  
113 of using radioisotopes before designing research studies.

114  
115 ~~This~~The main objective of this research paper ~~compares~~is to explore the use of  $^{137}\text{Cs}$ - and  $^{210}\text{Pb}$  to estimate recent OC  
116 sequestration rates in ~~intact~~undisturbed (i.e., not directly impaired by human activities) ~~freshwater mineral soil~~  
117 ~~wetlands~~temperate inland wetland soils located on agricultural landscapes. ~~Sediment cores were screened (to remove~~Here,  
118 we aim to (1) categorize  $^{137}\text{Cs}$  or  $^{210}\text{Pb}$  profiles ~~with evidence of vertical mixing~~),into high- and ~~then~~low-quality via a  
119 decision framework, (2) apply the ~~remaining profiles were used~~decision framework to estimate OC sequestration rates ~~using~~,  
120 (3) use 1963 and 1954 time-markers to compare the  $^{137}\text{Cs}$ -~~or~~ and  $^{210}\text{Pb}$ -~~radioisotope dating~~.~~The~~-based OC sequestration  
121 rates ~~based on  $^{137}\text{Cs}$  vs.  $^{210}\text{Pb}$  and based on the onset (1954) or peak (1963)~~to get a better understanding of the sediment  
122 history, and (4) select the best approach for  $^{137}\text{Cs}$  ~~radioisotope activity were then compared~~and  $^{210}\text{Pb}$  to estimate the OC  
123 sequestration rates with highest precision. This study helps reduce uncertainty in studies that rely on  $^{137}\text{Cs}$  or  $^{210}\text{Pb}$   
124 radioisotope dating.

## 125 2 Methods

### 126 2.1 Sediment core collection

127 Triplicate sediment cores were collected from 30 ~~intact freshwater mineral soil wetlands~~undisturbed temperate inland  
128 wetland soils in agricultural landscapes across southern Canada (~~Supplementary~~Fig. 1). A summary of the physical  
129 characteristics of these wetlands can be found in Supplementary Table 1. These wetlands were ~~intact~~undisturbed, with no  
130 known history of cultivation. The sediment cores were extracted from the center of the wetland, constituting the open-water  
131 area. A Watermark Universal Corer (inner diameter of 6.8 cm) ~~and/or~~ VibeCore Mini with poly core tubes (inner diameter of  
132 7.6 cm) were used to collect most of the sediment cores. A JMP BackSaver Soil sampler (inner diameter of 3.8 cm) was used  
133 for compacted sediment cores. Shallow (15 to 90 cm) sediment cores were sectioned into 1- or 2-cm increments. Deeper (>  
134 90 cm) sediment cores were sectioned into 5-cm increments. The sediment cores were stored at -5 °C for further processing  
135 at the laboratory.



136  
 137 **Figure 1: (a) Study area situated in four provinces of Canada; (b) three wetland sites in Alberta (AB); (c) three wetland sites in**  
 138 **Ontario (ON); (d) seven wetland sites in Saskatchewan (SK); (e) nine wetland sites in Saskatchewan (SK); (f) five wetland sites in**  
 139 **Manitoba (MB); and (g) three wetland sites in Ontario (ON). Figures (b)-(g) are based on the sampling locations of wetlands used in**  
 140 **this study reproduced using Google Earth Images [(b) and (c) ©2024 Airbus; (d), (e), and (g) ©2024 Maxar Technologies; (f) ©2024**  
 141 **Airbus and Maxar Technologies].**

## 2.2 Generation of $^{137}\text{Cs}$ and $^{210}\text{Pb}$ profiles

Sediment core increments were weighed (wet mass), dried, weighed again (dry mass), disaggregated, homogenized, and sieved. The increments were sieved to remove gravel (> 2 mm); radioisotopes do not bind on the gravel, and gravel does not contain OC; therefore, ~~removing~~eliminating gravel improves the estimate of radioisotopes and OC. The increments were counted at 661.6 keV for  $^{137}\text{Cs}$  activity and 46.5 keV for ~~and~~ $^{210}\text{Pb}$  activity.  $^{137}\text{Cs}$  analysis was performed using a gamma spectrometer, and  $^{210}\text{Pb}$  analysis was performed using both gamma and alpha spectrometers to increase throughput rates. The gamma analysis was conducted using the high-purity germanium detectors; e.g., Broad Energy Germanium detectors (BE6530) and ~~high resolution~~ Small Anode Germanium well detectors (GSW275L) (Mirion Technologies, Inc., Atlanta, GA, USA). The alpha analysis was conducted using ORTEC® alpha spectrometer (AMETEK® Advanced Measurement Technology, TN, USA). Both radioisotope analyses were performed at the Landscape Dynamics Laboratory, University of Manitoba, Winnipeg, Canada. Although the underlying principles of gamma and alpha analysis differ, each focuses on quantifying the decay of  $^{210}\text{Pb}$ , generating comparable results (Zaborska et al., 2007). ~~Measurement accuracy of gamma detectors is ensured by assessing the counting errors with reference materials within the same geometry as the sample (e.g., petri dish). Detection error was < 10% with a counting time of up to 24 h. Furthermore, Landscape Dynamics Laboratory undergoes regular Proficiency Testing through the International Atomic Reference Material Agency (IARMA) and previously through the International Atomic Energy Agency (IAEA) to ensure acceptable accuracy and precision of analytical results using gamma spectroscopy.~~

## 2.3 Screening of $^{137}\text{Cs}$ and $^{210}\text{Pb}$ profiles

Sediment cores were screened to remove profiles with evidence of vertical mixing, and then the remaining profiles were used to estimate OC sequestration rates using  $^{137}\text{Cs}$  or  $^{210}\text{Pb}$  radioisotope dating. The actual  $^{137}\text{Cs}$  peak can vary from the expected peak, increasing uncertainty in  $^{137}\text{Cs}$  dating (Drexler et al., 2018).  $^{137}\text{Cs}$  peaks can be “noisy” or “disturbed”; i.e., flattened, broadened, truncated, mixed, fluctuating (Drexler et al., 2018), or one-sided where the  $^{137}\text{Cs}$  peaks appear at the surface of the sediment core (indicating no or little sedimentation since 1963). ~~Such noise in  $^{137}\text{Cs}$  peaks can be caused by diffusion, disturbance, removal, and receiving  $^{137}\text{Cs}$  enriched sediments (Anderson et al., 1987; Milan et al., 1995; Jagereikova et al., 2015).~~The magnitude and shape of the  $^{137}\text{Cs}$  peaks observed in the sediments can be affected by the atmospheric deposition rate of  $^{137}\text{Cs}$ , which is obviously affected by the number and magnitude of emission events and the weather conditions following these events (UNSCEAR, 2000). The magnitude and shape of these peaks are also impacted by the movement of water and sediment within each wetland's catchment during the peaks' development (Milan et al., 1995; Zarrinabadi et al., 2023). Here, changes in the shape of the peaks are caused by the upward and downward movement of the sediment within the sediment profile (the movement of  $^{137}\text{Cs}$  through diffusion (Klaminder et al., 2012) is presumed negligible). Bioturbation can cause an upward and downward mixing of the  $^{137}\text{Cs}$  in the profile, resulting in peak attenuation (Robbins et al., 1977).



173 Even wave action during the period of atmospheric deposition will have a similar attenuation effect (Andersen et al., 2000;  
174 Zarrinabadi et al., 2023). Following peak atmospheric deposition, soil erosion and the accumulation of sediment will deliver  
175 sediments to the top of the profile, and those sediments may be higher or lower in concentration depending on the degree of  
176 preferential sediment transport and the associated enrichment or depletion of  $^{137}\text{Cs}$  in the added sediment (Zarrinabadi et al.,  
177 2023). Such noise in  $^{137}\text{Cs}$  peaks needs careful interpretation to avoid over- or under-estimating the OC sequestration rates.

178  
179 *Selecting suitable cores:* Of the 90 sediment cores, (30 wetlands x 3 replicates = 90), 79 were suitable (complete and datable)  
180 for  $^{137}\text{Cs}$  dating and 47 ~~were suitable~~ for  $^{210}\text{Pb}$  dating. ~~Suitability~~ Only some replicates from the same wetland were ideal for  
181 interpretation or further screening. The suitability of  $^{137}\text{Cs}$  profiles for dating was assessed by zero activity before the onset  
182 and ~~the~~ peak of  $^{137}\text{Cs}$  activity. The suitability of  $^{210}\text{Pb}$  profiles for dating was ~~assessed~~ evaluated by determining the  
183 exponential decline in  $^{210}\text{Pb}$  activity with depth until background levels are reached.

184  
185 *Classification of the selected  $^{137}\text{Cs}$  profiles:* The 79 suitable  $^{137}\text{Cs}$  profiles were then classified into high- and low-quality  
186 using the following steps (Fig. ~~1a~~2a):

- 187  
188 1. The  $^{137}\text{C}$  depth profile and the shape of the peak were assessed. ~~The presence of a~~ A clear and distinct peak  
189 associated with several points on both sides of the peak verified the  $^{137}\text{Cs}$  depth profile as high-quality- (e.g., Fig.  
190 3a).
- 191 2. When analyzing sediment samples, a clear peak in  $^{137}\text{Cs}$  activity didn't always exist- (e.g. Fig 4a). If a peak was  
192 absent, which could have resulted from sediment influxes with very high or very low  $^{137}\text{Cs}$  activity levels, the total  
193  $^{137}\text{Cs}$  activity of the entire profile was examined. If the cumulative  $^{137}\text{Cs}$  inventory value for the entire profile was  $\geq$   
194  $500 \text{ Bq m}^{-2}$ , then the  $^{137}\text{Cs}$  profile was considered ~~as~~ high-quality. Conversely, if the cumulative  $^{137}\text{Cs}$  inventory  
195 value for the entire profile was  $< 500 \text{ Bq m}^{-2}$ , ~~then~~ the  $^{137}\text{Cs}$  profile was considered ~~as~~ low-quality. The cutoff  
196 cumulative  $^{137}\text{Cs}$  inventory value of  $500 \text{ Bq m}^{-2}$  was established by assessing the  $^{137}\text{Cs}$  reference inventory value,  
197 the value of  $^{137}\text{Cs}$  present in a non-eroded system with an undisturbed profile. The  $^{137}\text{Cs}$  reference inventory value  
198 differs from region to region (Owens and Walling, 1996), and the most proximal regional value was used to select  
199 the cutoff  $^{137}\text{Cs}$  inventory value (Sutherland, 1991; Kachanoski and Von Bertoldi, 1996; Zarrinabadi et al., 2023).  
200 The  $^{137}\text{Cs}$  reference inventory is a catchment-wide reference value and not specific to the wetland center; thus, the  
201 cumulative  $^{137}\text{Cs}$  inventory value of  $500 \text{ Bq m}^{-2}$  was viewed as a conservative indicator of the suitability of the  $^{137}\text{Cs}$   
202 profiles. Ideally, reference sites are large, open, level, non-eroded areas, usually in forage or grassland since the  
203 1950s, and within 10 km of the site of interest. In this study, it was impossible to identify a suitable reference site  
204 near every wetland; it is usually difficult to find reference sites in agricultural landscapes. However, we could locate

205 reference sites used in other studies within 50 km except from nine wetlands in SK (51° N and 104° W), which  
206 were ~150 km from the reference site. Although this was not considered ideal, it was considered acceptable.

207  
208 *Classification of the selected <sup>210</sup>Pb profiles:* The 47 suitable <sup>210</sup>Pb profiles were classified into high- and low-quality profiles  
209 based on the following steps (Fig. 1b2b):

- 211 1. <sup>210</sup>Pb activity were plotted with a log-transformed <sup>210</sup>Pb<sub>ex</sub> against mass depth (g cm<sup>-2</sup>).
- 212 2. A linear regression analysis was performed (where the slope is used to derive the mass or sediment accumulation  
213 rate in g cm<sup>-2</sup> yr<sup>-1</sup>).
- 214 3. If the linear regression passed both normality and constant variance tests and had an R<sup>2</sup> > 0.5 and a p-value < 0.05,  
215 then the <sup>210</sup>Pb profile was classified as high-quality (e.g., Fig. 3a).
- 216 4. If either of the normality and constant variance tests were not passed, had with an R<sup>2</sup> ≤ 0.5, or a p-value ≥ 0.05, then  
217 the <sup>210</sup>Pb profile was considered low-quality (e.g., Fig. 3b).

218  
219 The <sup>210</sup>Pb profiles were also classified based on using a two-step piecewise linear regression model to capture recent shifts in  
220 OC sequestration rates. However, no significant improvement was observed. Consequently, <sup>210</sup>Pb-based OC sequestration  
221 rates were derived from the linear regression line. An R<sup>2</sup> > 0.5 was selected as the cut-off for selecting high-quality over low-  
222 quality profiles. Increasing the cut-off R<sup>2</sup> value may produce better profiles to be selected chosen for the study but. Still, it  
223 can reduce the number of available sediment cores for the study and potentially ignore the natural variability and significant  
224 events occurring in the real environment.

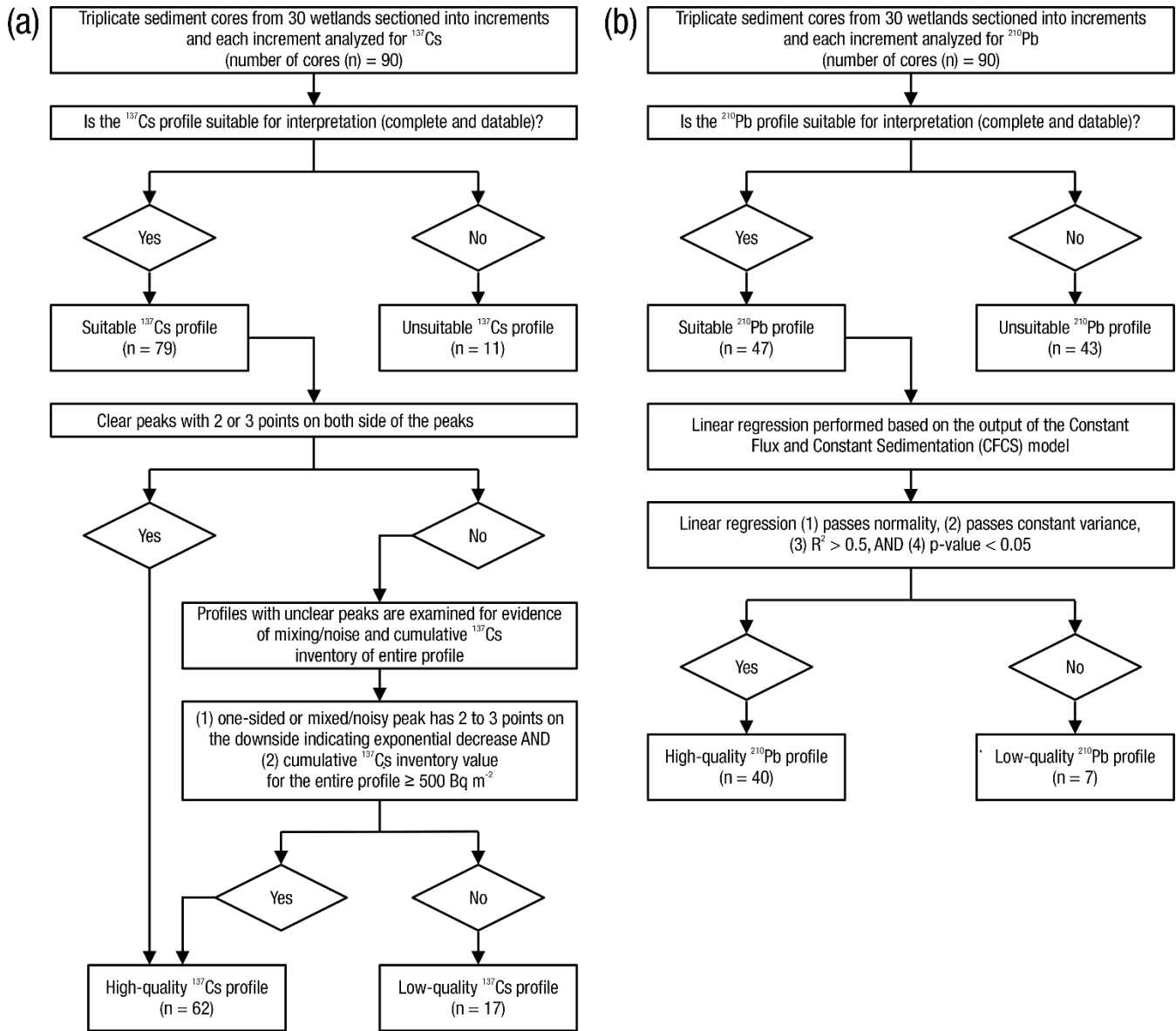


**Figure 12:** Classification of high- and low-quality  $^{137}\text{Cs}$  and  $^{210}\text{Pb}$  profiles outlining the decision frameworks for screening (a)  $^{137}\text{Cs}$  profiles and (b)  $^{210}\text{Pb}$  profiles.

## 2.4 ~~OC~~Organic carbon stocks and sequestration rates

Radioisotope activity measurements were utilized to assign two time-markers, one for 1954 and the other for 1963, in the sediment cores. Sediment radioisotope dating was used to calculate the rates of sediment or mass accumulation and OC sequestration.

For  $^{137}\text{Cs}$  dating, sediment accumulation and OC sequestration rates ( $\text{Mg ha}^{-1} \text{ yr}^{-1}$ ) were estimated using the cumulative sum of sediment or OC ( $\text{Mg ha}^{-1}$ ) from the surface to the depth corresponding to the time-markers of  $^{137}\text{Cs}$  of each core and dividing by the number of years from the time-marker to the years the samples were collected. Unit conversion is applied to report the OC sequestration rate estimates in  $\text{Mg ha}^{-1} \text{ yr}^{-1}$  from  $\text{g cm}^{-2} \text{ yr}^{-1}$  for easy standardization and comparability with other studies. For  $^{137}\text{Cs}$  profiles with noisy peaks and comparatively larger cumulative  $^{137}\text{Cs}$  inventory values, the first elongated peak with a sharp rise after the onset of the  $^{137}\text{Cs}$  peak was considered the 1963 peak instead of the peak with the highest activity in the profile.

For  $^{210}\text{Pb}$  dating, mass or sediment accumulation and OC sequestration rates were estimated using the Constant Flux and Constant Sedimentation (CFCS) model (Sanchez-Cabeza and Ruiz-Fernandez, 2012; Kamula et al., 2017). Here,  $^{210}\text{Pb}_{\text{ex}}$  was estimated by subtracting  $^{226}\text{Ra}$  activity (186 keV) from the total  $^{210}\text{Pb}$  activity. The CFCS model uses the log-linear relationship of  $^{210}\text{Pb}_{\text{ex}}$  with mass depth and converts  $^{210}\text{Pb}_{\text{ex}}$  to the mass or sediment accumulation rate and, consequently, the OC sequestration rate. The OC stock was estimated by taking the cumulative sum of OC ( $\text{Mg ha}^{-1}$ ) from the surface of each sediment core to the depth increments represented by the time-marker (e.g., 1963).

OC stocks for the 1954 and 1963 time-markers were calculated by multiplying the OC content per unit mass of soil ( $\text{g g}^{-1}$ ). Here, OC content was calculated from OC concentration in-%(%) measured by loss-on-ignition (LOI) method (Kolthoff and Sandell, 1952) by the mass of sediment for each section interval and specific depth interval per unit area ( $\text{g cm}^{-2}$ ) down the profile to the respective time-marker. OC (%) was calculated by multiplying organic matter (%) by LOI with 0.58, assuming 58% of the organic matter is carbon. Despite the broad applicability, simplicity in measurement techniques, and cost-effectiveness, the LOI approach is associated with some limitations, such as the ignition of non-organic particles at high temperatures or the use of a conventional conversion factor (Pribyl, 2010; Hoogsteen et al., 2015), which can result in over-estimation of OC content.

## 2.5 Statistical analysis

Statistical analyses were conducted using used sediment cores where both with  $^{137}\text{Cs}$ - and  $^{210}\text{Pb}$ -based OC sequestration rates were available. (number of sediment cores ( $n$ ) = 44). The  $^{137}\text{Cs}$ —and  $^{210}\text{Pb}$ -based estimates of OC sequestration rates were

260 compared using a quantile-quantile (Q-Q) plot. First, the comparison was done via assessment of the Q-Q plots. Four sample  
261 datasets were used to construct Q-Q plots to compare the distribution of <sup>137</sup>Cs- and <sup>210</sup>Pb-based OC sequestration against the  
262 1:1 line.

263  
264 The sample datasets included:

- 265  
266 • D1, all suitable <sup>137</sup>Cs and <sup>210</sup>Pb profiles with OC sequestration rates estimated since 1954 (~~number of sediment cores~~  
267 ~~(n)~~n = 44).
- 268 • D2, all suitable <sup>137</sup>Cs and <sup>210</sup>Pb profiles with OC sequestration rates estimated since 1963 (n = 44).
- 269 • D3, high-quality <sup>137</sup>Cs and <sup>210</sup>Pb profiles with OC sequestration rates estimated since 1954 (n = 30).
- 270 • D4, high-quality <sup>137</sup>Cs and <sup>210</sup>Pb profiles with OC sequestration rates estimated since 1963 (n = 30).

271  
272 A Q-Q plot was calculated for each dataset. The x- and y- coordinates of a point in a Q-Q plot corresponded to the  $p^{\text{th}}$   
273 percentiles of the two OC sequestration rate estimates ~~that were~~ being compared in the plot. Here,  $p = (k - 0.5) / n$ , where n  
274 is the sample size and  $k = 1, \dots, n$  (Jain et al., 2007). ~~To assess whether the two OC sequestration rate estimates are similar,~~  
275 ~~the~~The distribution of the points on the Q-Q plot was compared against the  $y = x$  (1:1) line to assess whether the two OC  
276 sequestration rate estimates are similar. If the points were distributed in a straight line and close to a 1:1 line, then it  
277 suggested that the two estimates came from the same distribution. In contrast, if the points were not distributed in a straight  
278 line or deviated from the 1:1 line, then it suggested that the two estimates did not come from the same distribution. The Q-Q  
279 plots were generated in Microsoft Excel (Microsoft 365, Version 2402, Redmond, WA).

280  
281 Since interpreting the Q-Q plot through a visual inspection can be subjective to human perception, we compared the <sup>137</sup>Cs-  
282 and <sup>210</sup>Pb-based OC sequestration rate estimates using a distance sampling model. A distance sampling model captures how  
283 the detectability of objects from the observer (walking along a straight line) decreases with the increase in the object-to-  
284 observer distance. If the objects are closely distributed along the ~~observer's path-of-the-observer~~ (i.e., if points of the Q-Q  
285 plot were closely distributed along the 1:1 line), then the distribution of the distances is expected to be a half normal  
286 distribution. The Cramer-von Mises test was used to estimate whether the distances ( $q_1, q_2, \dots, q_n$ ) from the points to the  
287 1:1 line were from a half-normal distribution. Given a set of distance samples ( $q_1, q_2, \dots, q_n$ ) and a detection function, the  
288 Cramer-von Mises test builds a model that fits the distance sampling data to the detection function (for details on modelling,  
289 see Miller et al., 2019). A half-normal key is commonly used as a detection function, corresponding to a half-normal  
290 distribution's shape.

291

292 The Cramer-von Mises test produced a p-value and Akaike's Information Criterion (AIC) as its test statistic. A p-value larger  
293 than the significant level ( $p = 0.05$ ) indicated that the likelihood of points being observed closer to the 1:1 line is high, and  
294 that the **likelihood probability** decreases as the distances increase. This provided evidence of the points being closely  
295 distributed along the 1:1 line. The AIC was used to rank the distance sampling models, which are built by the Cramer-von  
296 Mises test, from best to worst (e.g., Burnham and Anderson, 2003); a small AIC value indicates a good fit to the half-normal  
297 key and thus provides evidence that the points are close to the 1:1 line (Miller et al., 2019). The distance sampling Cramer-  
298 von Mises test was computed using the "distance" package in R version 4.0.3 (Miller and Clark-Wolfe, 2023; R Core Team,  
299 2023).

### 300 **3 Results**

#### 301 **3.1 High- and low-quality $^{137}\text{Cs}$ and $^{210}\text{Pb}$ profiles**

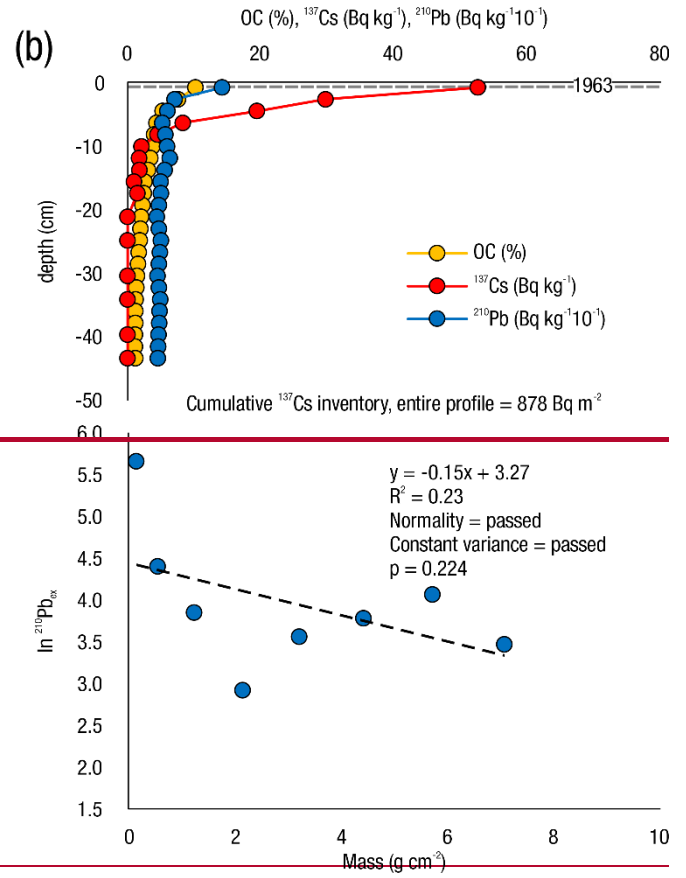
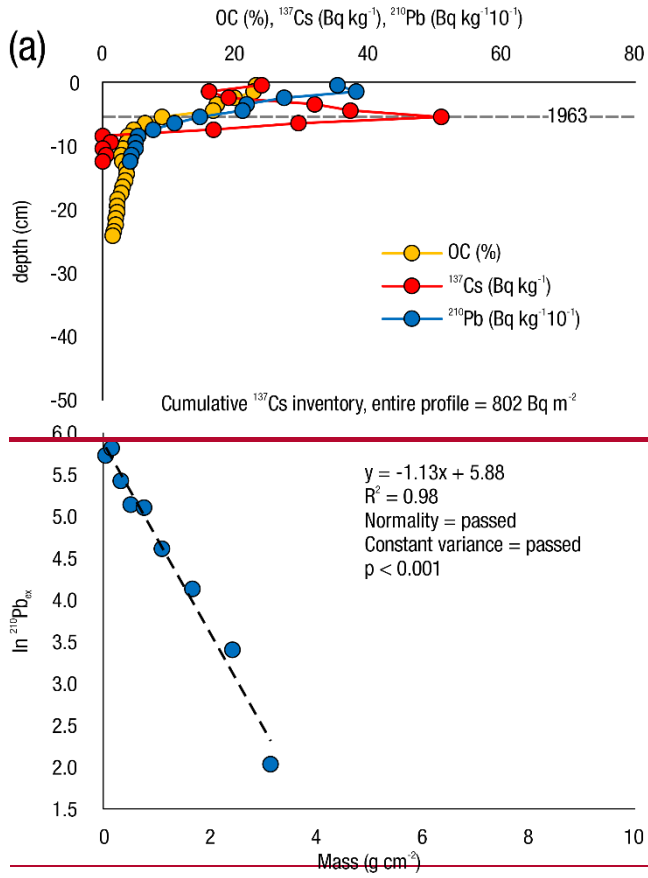
302 Of the 79 suitable  $^{137}\text{Cs}$  profiles, 62 (78%) were classified as **being of** high-quality. Of the 62 high-quality  $^{137}\text{Cs}$  profiles,  
303 61% had clear and distinct peaks, with a smooth rise and decline, **while**. **In contrast**, the remaining 39% had noise—either  
304 one-sided peaks or disturbed peaks. (e.g., Fig. 4). Of the 62 high-quality  $^{137}\text{Cs}$  profiles, 4 (6.5%) were repositioned to capture  
305 the  $^{137}\text{Cs}$  enriched sediments post 1963. (e.g.,  $^{137}\text{Cs}$  profile of S-LO-I-W4-T2-CW-R2 in Supplementary Fig. 2a). In these  
306 profiles, which had a cumulative  $^{137}\text{Cs}$  inventory value  $> 1,200 \text{ Bq m}^{-2}$ , the depth that corresponded to  $^{137}\text{Cs}$  cumulative  
307 inventory value of  $\sim 500 \text{ Bq m}^{-2}$  was considered as the 1963 time-marker. **The high total quantities of  $^{137}\text{Cs}$  profile**  
308 **inventories can be attributed to receiving  $^{137}\text{Cs}$  enriched sediments from the surrounding landscape. Sediments that have**  
309 **undergone substantial preferential detachment and entrainment on their pathway into a wetland can have very high**  
310 **concentrations of  $^{137}\text{Cs}$  and, when interlayered with sediments that are not so enriched, can generate multiple  $^{137}\text{Cs}$  peaks in**  
311 **the sediment profile peaks after 1963. These observed multiple peaks are local and not regional, ruling out the association**  
312 **with Chernobyl and Fukushima events. Two  $^{137}\text{Cs}$  profiles were considered high-quality despite a cumulative  $^{137}\text{Cs}$  inventory**  
313 **value  $< 500 \text{ Bq m}^{-2}$  because the 1963 peak was clear, distinct, and elongated with two-to-three points on both sides of the**  
314 **peak. (e.g.,  $^{137}\text{Cs}$  profile of M-OA-I-W4-T2-CW-R2 in Supplementary Fig. 7b). One  $^{137}\text{Cs}$  profile was considered high-**  
315 **quality despite showing marginal quality to the set criteria in the decision framework, where the peak profile had good shape**  
316 **with several points on the downside of the peak and one point on the other side and had a cumulative  $^{137}\text{Cs}$  inventory value**  
317 **of  $499 \text{ Bq m}^{-2}$ . One  $^{137}\text{Cs}$  profile was classified as low-quality despite a cumulative  $^{137}\text{Cs}$  inventory value  $> 500 \text{ Bq m}^{-2}$**   
318 **because the peak was highly fluctuating and not discernible. (e.g.,  $^{137}\text{Cs}$  profile of O-AL-I-W6-T1-CW-R1 in Supplementary**  
319 **Fig. 12b).**

320

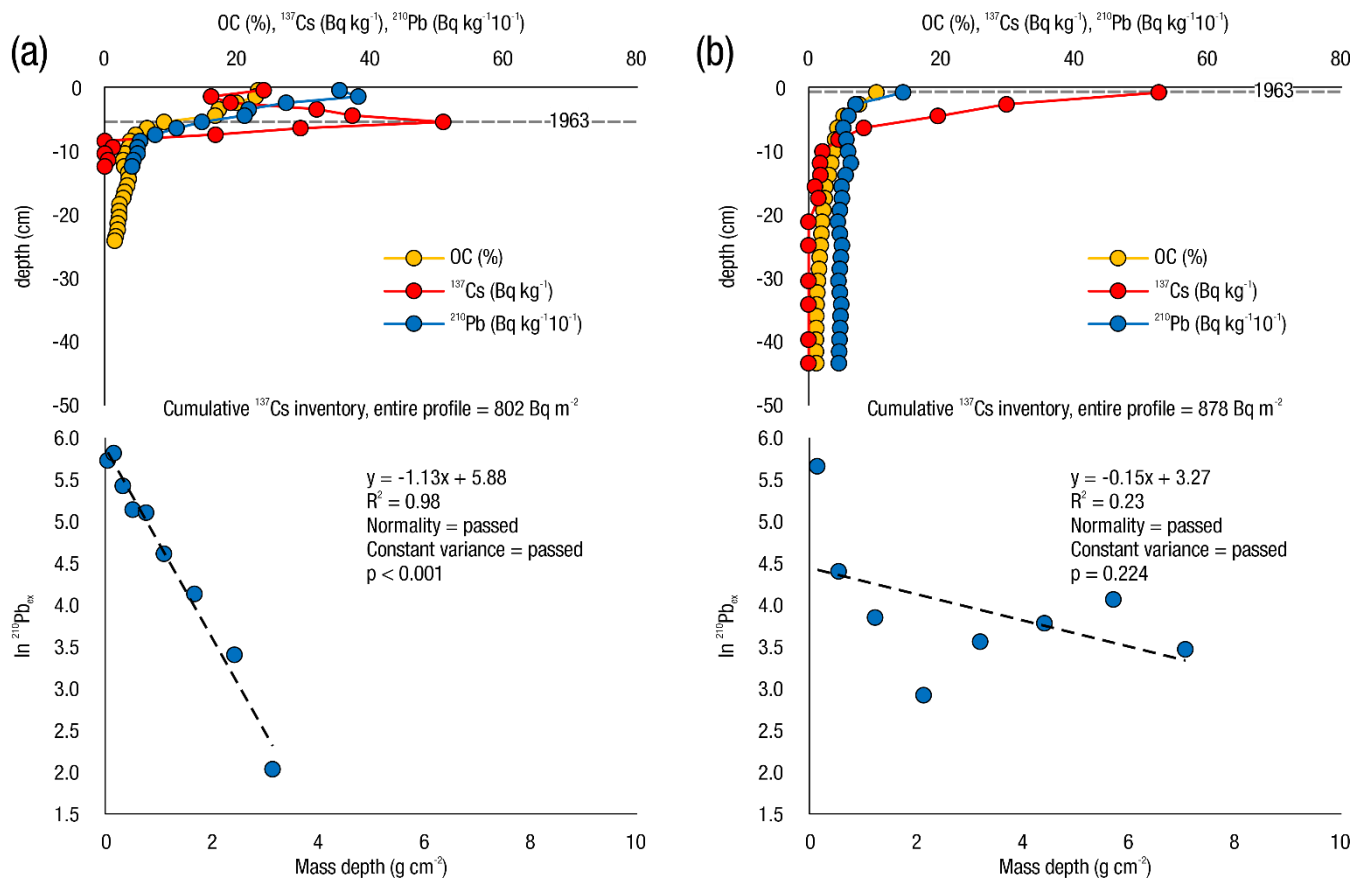
321 Of the 47  $^{210}\text{Pb}$  profiles, 40 (85%) were classified as high-quality.

322

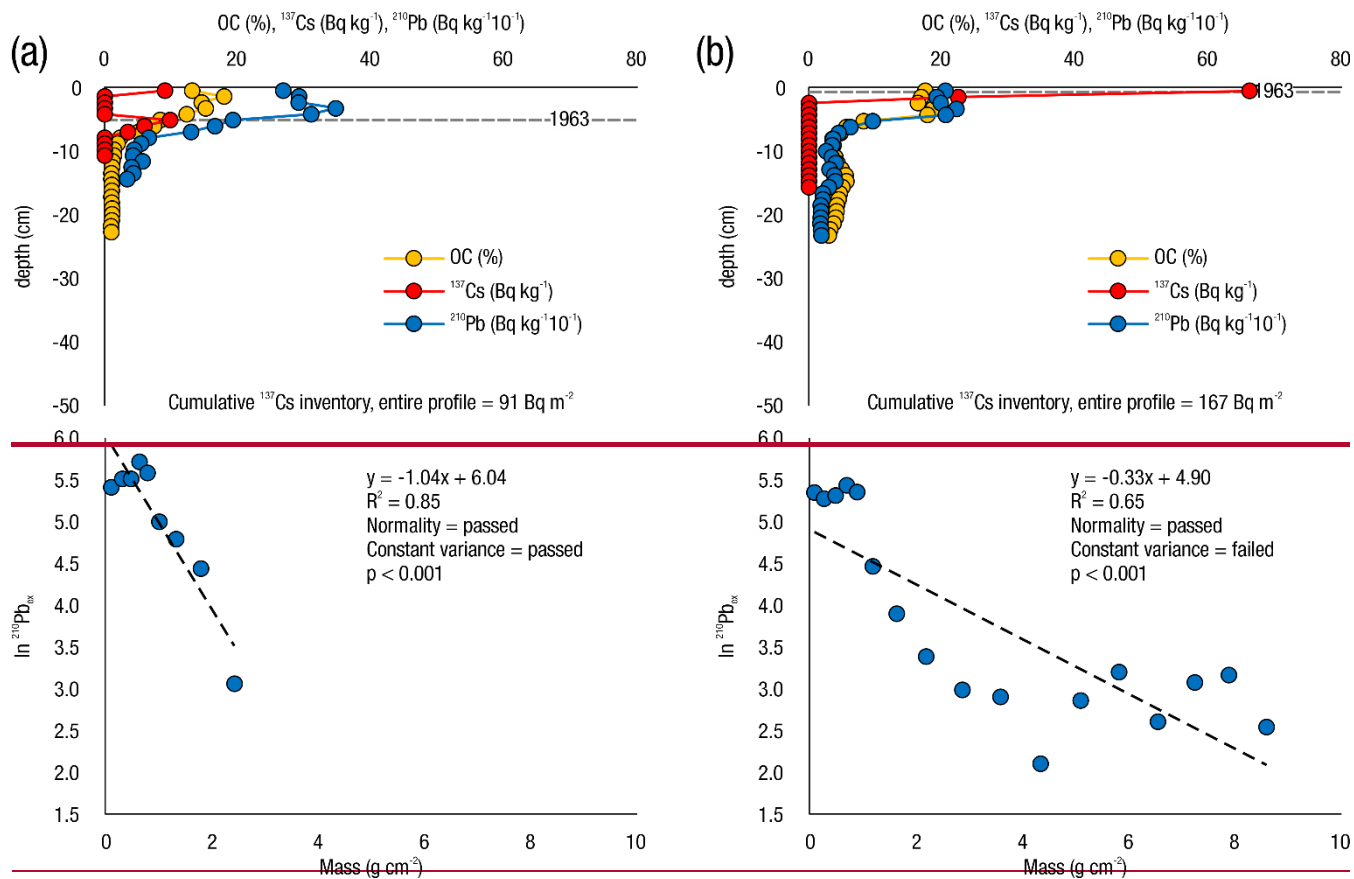
323 There were 44 sediment cores with both  $^{137}\text{Cs}$  and  $^{210}\text{Pb}$  suitable profiles available. Of these, 30 were categorized as high-  
324 quality  $^{137}\text{Cs}$  and high-quality  $^{210}\text{Pb}$  (Fig. ~~2a~~, ~~63a~~), six were categorized as high-quality  $^{137}\text{Cs}$  and low-quality  $^{210}\text{Pb}$  (Fig.  
325 ~~2b~~, ~~73b~~), seven were ~~categorized~~ classified as low-quality  $^{137}\text{Cs}$  and high-quality  $^{210}\text{Pb}$  (Fig. ~~3a~~4a), and ~~1~~one was categorized  
326 as low-quality  $^{137}\text{Cs}$  and low-quality  $^{210}\text{Pb}$  (Fig. ~~3b~~4b). (See Supplementary Figs. ~~2~~1 to ~~13~~12 for  $^{137}\text{Cs}$  and  $^{210}\text{Pb}$  profiles in all  
327 study wetlands.)



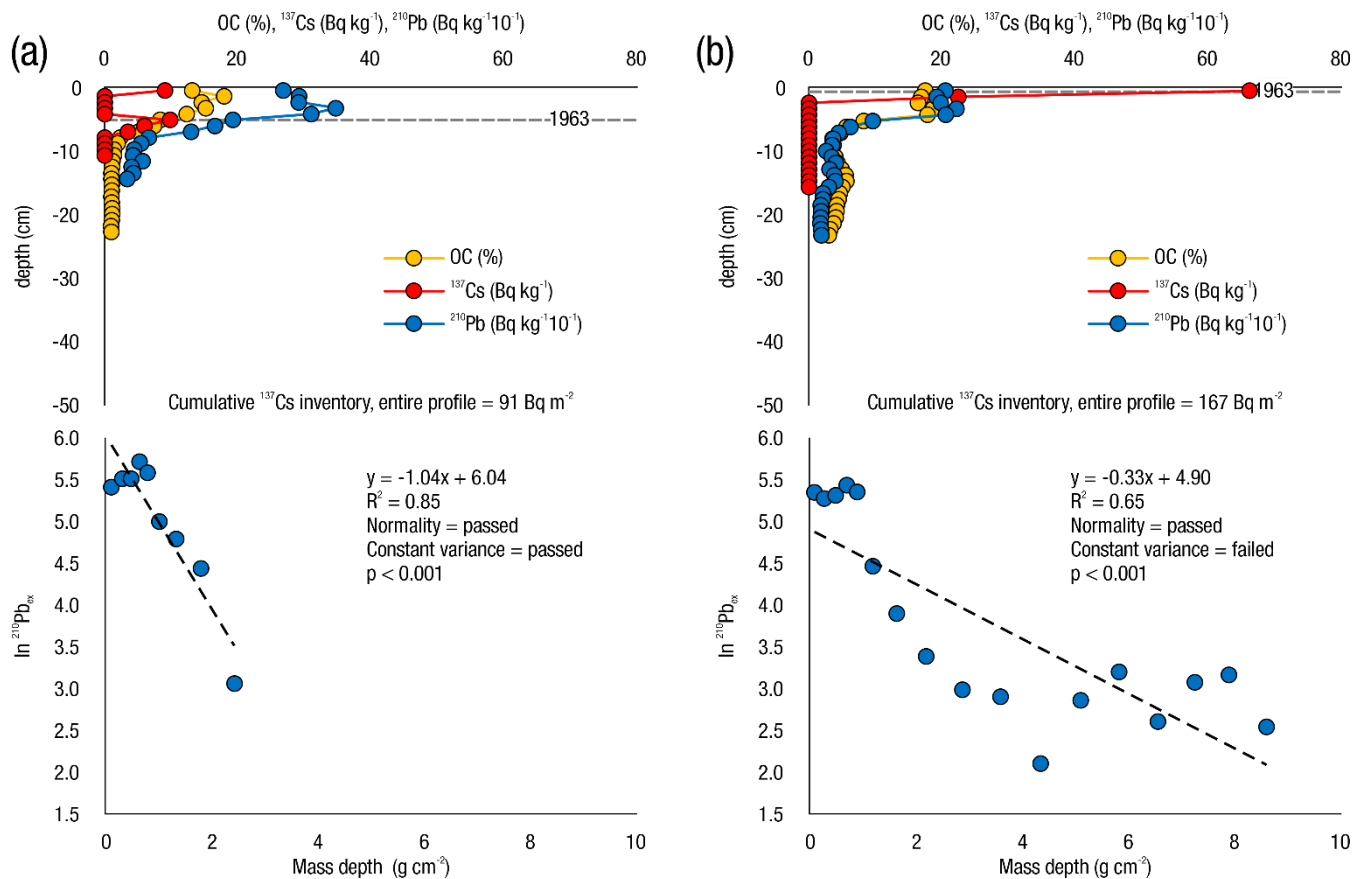




330  
 331 **Figure 2: Examples of  $^{137}\text{Cs}$  and  $^{210}\text{Pb}$  classifications showing OC (%),  $^{137}\text{Cs}$  ( $\text{Bq kg}^{-1}$ ), and  $^{210}\text{Pb}$  ( $\text{Bq kg}^{-1}$ ) depth profiles and plots**  
 332 **of log-transformed  $^{210}\text{Pb}_{\text{ex}}$  against mass ( $\text{g cm}^{-2}$ ): (a) high-quality  $^{137}\text{Cs}$  and high-quality  $^{210}\text{Pb}$  (SK-A3 T1); (b) high-quality  $^{137}\text{Cs}$  and**  
 333 **low-quality  $^{210}\text{Pb}$  (MB-4 T3).**



334  
 335 **Figure 3: Examples of  $^{137}\text{Cs}$  and  $^{210}\text{Pb}$  classifications showing OC (%),  $^{137}\text{Cs}$  ( $\text{Bq kg}^{-1}$ ), and  $^{210}\text{Pb}$  ( $\text{Bq kg}^{-1}$ ) depth profiles and plots**  
 336 **of log-transformed  $^{210}\text{Pb}_{\text{ex}}$  against mass depth ( $\text{g cm}^{-2}$ ): (a) low-high-quality  $^{137}\text{Cs}$  and high-quality  $^{210}\text{Pb}$  (SK-A1-T3); and S-LO-I-**  
 337 **W3-T1-CW-R1); (b) low-high-quality  $^{137}\text{Cs}$  and low-quality  $^{210}\text{Pb}$  (SK-A6-T1-M-OA-I-W4-T3-CW-R3).**

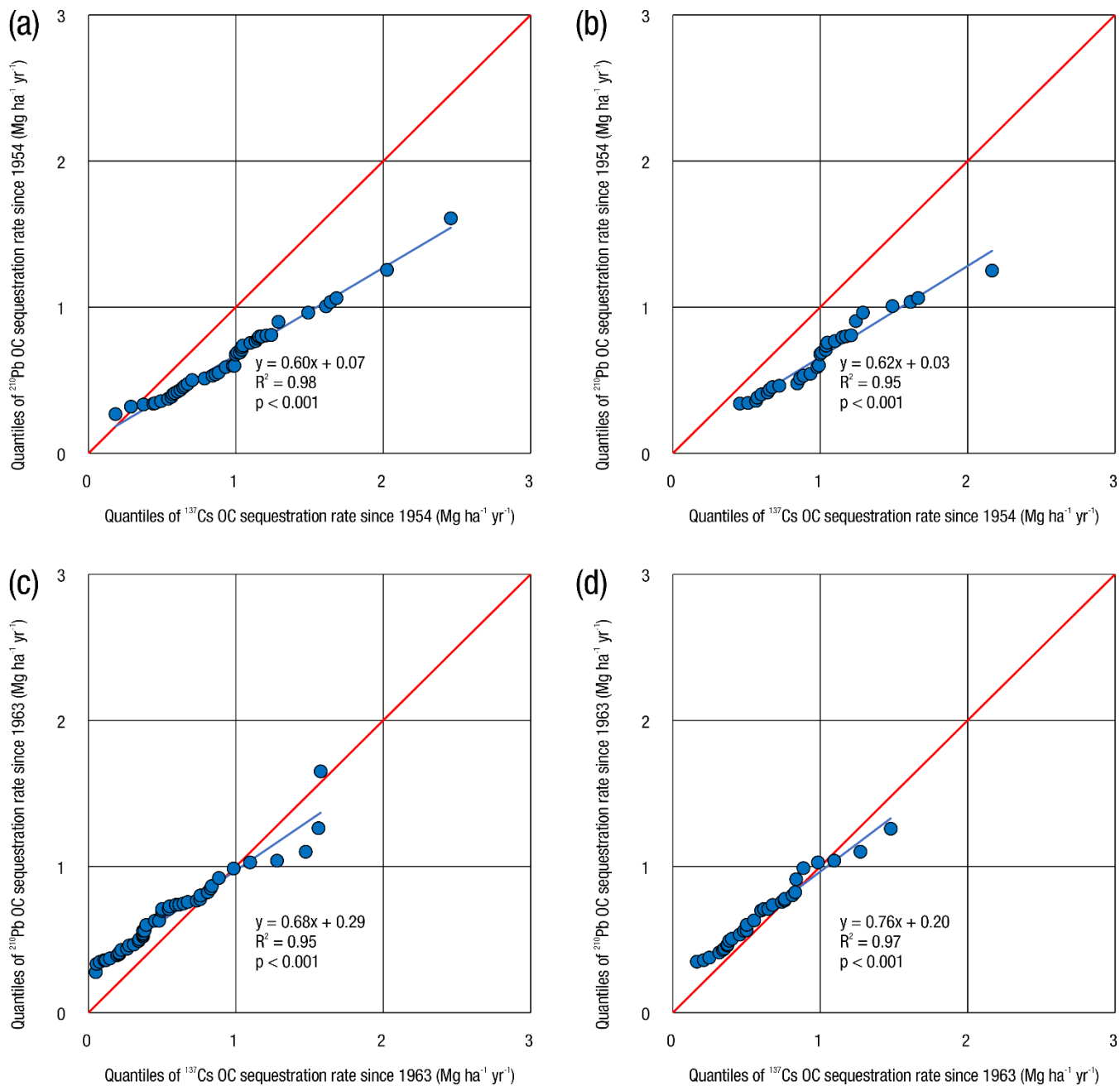


338  
 339 **Figure 4: Examples of  $^{137}\text{Cs}$  and  $^{210}\text{Pb}$  classifications showing OC (%),  $^{137}\text{Cs}$  ( $\text{Bq kg}^{-1}$ ), and  $^{210}\text{Pb}$  ( $\text{Bq kg}^{-1}$ ) depth profiles and plots**  
 340 **of log-transformed  $^{210}\text{Pb}_{\text{ex}}$  against mass depth ( $\text{g cm}^{-2}$ ): (a) low-quality  $^{137}\text{Cs}$  and high-quality  $^{210}\text{Pb}$  (S-RO-I-W1-T3-CW-R3); and**  
 341 **(b) low-quality  $^{137}\text{Cs}$  and low-quality  $^{210}\text{Pb}$  (S-RO-I-W6-T1-CW-R1).**

342 **3.2  $^{137}\text{Cs}$  vs.  $^{210}\text{Pb}$  derived ~~OC~~ organic carbon sequestration rates**

343 ~~The comparability of  $^{137}\text{Cs}$  vs.  $^{210}\text{Pb}$  derived OC sequestration rates was investigated through both visual inspection of the Q-~~  
 344 ~~Q plots and the Cramer von Mises test which assigned significance of the distance of the points from the 1:1 line assessed~~  
 345 ~~with p value and the AIC.~~

346  
 347 For each of the four datasets (D1-D4), the points on the Q-Q plot were distributed in a straight line, showing a linear  
 348 relationship between the two estimates being compared ( $R^2 > 0.95$ ,  $p\text{-value} < 0.001$ ) (Fig. 45).



349

350 **Figure 45:** Q-Q plot of  $^{137}\text{Cs}$ - vs.  $^{210}\text{Pb}$ -based organic carbon (OC) sequestration rates using (a) all suitable  $^{137}\text{Cs}$  and  $^{210}\text{Pb}$  profiles  
 351 estimated since 1954 (D1), (b) high-quality  $^{137}\text{Cs}$  and  $^{210}\text{Pb}$  profiles estimated since 1954 (D3), (c) all suitable  $^{137}\text{Cs}$  and  $^{210}\text{Pb}$  profiles  
 352 estimated since 1963 (D2), and (d) high-quality  $^{137}\text{Cs}$  and high-quality  $^{210}\text{Pb}$  profiles estimated since 1963 (D4).

Visual inspection of the Q-Q plots showed that the points for D2 (i.e., all suitable  $^{137}\text{Cs}$  and  $^{210}\text{Pb}$  profiles using the 1963 time-marker; Fig. 4e5c) and D4 (i.e., high-quality  $^{137}\text{Cs}$  and  $^{210}\text{Pb}$  profiles using the 1963 time-marker; Fig. 4d5d) were distributed more closely along the 1:1 line compared to that of D1 (i.e., all suitable  $^{137}\text{Cs}$  and  $^{210}\text{Pb}$  profiles using the 1954 time-marker; Fig. 4a5a) and D3 (i.e., high-quality  $^{137}\text{Cs}$  and  $^{210}\text{Pb}$  profiles using the 1954 time-marker; Fig. 4b5b).

An intercept closer to 0 and a slope closer to 1 indicated good alignment of the regression line to the 1:1 line. The slope (s) and intercept (i) of the regression lines were: s = 0.60, i = 0.07 for D1 (Fig. 4a5a); s = 0.62, i = 0.03 for D3 (Fig. 4b5b); s = 0.68, i = 0.29 for D2 (Fig. 4e5c); and s = 0.76, i = 0.20 for D4 (Fig. 4d5d). D2 and D4 had regression lines and slopes closer to the 1:1 line but intercepts further from the origin compared to than D1 and D3.

The Cramer-von Mises test was used to build distance sampling models using the point-to-1:1-line distances computed from the Q-Q plots. Models built with the D4 dataset produced the best-fit model (i.e., p-value > 0.05, AIC = -114). Models built with the D1, D2, and D3 datasets had weaker p-values (p-value < 0.05) and can be ranked based on lower AIC scores (AIC = -116 for D2, AIC = -54 for D1, and AIC = -34 for D3).

### 3.3 Sediment accumulation, $\Theta$ organic carbon sequestration rates and stocks

The 30 sediment cores (68% of all the suitable  $^{137}\text{Cs}$  and  $^{210}\text{Pb}$  profiles) with high-quality  $^{137}\text{Cs}$  and  $^{210}\text{Pb}$  profiles were used to calculate mass or sediment accumulation rates, OC sequestration rates, and OC stocks (Table 2). OC sequestration rates based on  $^{137}\text{Cs}$  and  $^{210}\text{Pb}$  dating estimated since 1954 and 1963 of 44 suitable sediment cores (where both  $^{137}\text{Cs}$  and  $^{210}\text{Pb}$  profiles were available) are presented in Supplementary Table 2.

**Table 2: Sedimentation accumulation, OC stocks, and sequestration rates of intact undisturbed wetlands estimated using high-quality  $^{137}\text{Cs}$  and high-quality  $^{210}\text{Pb}$  profiles.**

Type of radiometric dating	$^{137}\text{Cs}$		$^{210}\text{Pb}$	
	1954	1963	1954	1963
Time-marker				
Range of accumulated sediment (Mg ha <sup>-1</sup> )	214-1,727	56-1,272	111-1,014	95-874
Mean (standard deviation) stock of OC (Mg ha <sup>-1</sup> )	66 (29)	35 (19)	43 (18)	38 (15)
Mean (standard deviation) rate of OC sequestration (Mg ha <sup>-1</sup> yr <sup>-1</sup> )	1.02 (0.44)	0.63 (0.34)	0.67 (0.27)	0.68 (0.26)

375 ~~The~~Based on the 1954 time-marker, the total sediment accumulation ~~based on the 1954 time marker~~ ranged from 214-1,727  
376 Mg ha<sup>-1</sup> using <sup>137</sup>Cs dating and 111-1,014 Mg ha<sup>-1</sup> using <sup>210</sup>Pb dating. In contrast, the total sediment accumulation based on  
377 the 1963 time-marker was lower, ranging from 56-1272 Mg ha<sup>-1</sup> using <sup>137</sup>Cs and 95-874 Mg ha<sup>-1</sup> using <sup>210</sup>Pb dating.  
378

379 The <sup>137</sup>Cs--derived mean OC sequestration rate was almost two times larger, at 1.02 Mg ha-1 yr-1 using the 1954 time-  
380 marker compared to 0.63 Mg ha-1 yr-1 using the 1963 time- marker. The corresponding <sup>137</sup>Cs-based mean OC stocks were  
381 66 Mg ha<sup>-1</sup> for 1954 and 35 Mg ha<sup>-1</sup> for 1963 (Table 2).  
382

383 The <sup>210</sup>Pb-derived mean OC sequestration rate was similar at 0.67 Mg ha<sup>-1</sup> yr<sup>-1</sup> using the 1954 time-marker compared to 0.68  
384 Mg ha<sup>-1</sup> yr<sup>-1</sup> using the 1963 time-marker. <sup>210</sup>Pb-based OC sequestration rates show minimal variation since they were  
385 calculated using the same sedimentation rate. The corresponding mean OC stocks were 43 Mg ha<sup>-1</sup> for the 1954 time-marker  
386 and 38 Mg ha<sup>-1</sup> for the 1963 time-marker, with a variable depth.  
387

388 ~~The~~Figure 3 and Supplementary Figs. 1 to 12 present the depth distributions of <sup>137</sup>Cs and <sup>210</sup>Pb activity (along with the  
389 linear plot of log-transformed <sup>210</sup>Pbex against mass depth in g cm-2) of all suitable profiles (n = 44) where both  
390 radioisotope profiles are available ~~are presented in Fig. 2 and Supplementary Figs. 2 to 13.~~

#### 391 4 Discussion

392 This study compared <sup>137</sup>Cs and <sup>210</sup>Pb dating for OC estimates in wetlands that were ~~intact~~undisturbed (i.e., without direct  
393 impact human activities) since both radioisotopes dating are known to provide reliable ~~estimates~~forecasts for recent OC  
394 sequestration rates (i.e., post-1954, which coincides with the onset of <sup>137</sup>Cs atmospheric deposition) (Drexler et al., 2018;  
395 Creed et al., 2022).  
396

397 This study highlights some ~~of the~~advantages and disadvantages of using <sup>137</sup>Cs vs. <sup>210</sup>Pb dating. For example, the  
398 ~~significantly~~smaller number of suitable <sup>210</sup>Pb profiles (47/90 = 52%) due to ~~the~~ lack of a complete decay profile (~~following~~  
399 ~~the~~ CFCS model as described in Sanchez-Cabeza and Ruiz-Fernandez, 2012) indicates that <sup>210</sup>Pb dating is more prone to  
400 disturbance than <sup>137</sup>Cs (79/90 = 88%). For <sup>137</sup>Cs, even if the sediment core is disturbed, estimation of OC sequestration rates  
401 may be possible with careful interpretation (e.g., see Fig. 42). The larger number of sediment cores using <sup>137</sup>Cs dating can be  
402 beneficial in accurately representing the heterogeneity of OC sequestration rates as it provides a larger dataset (a 36% gain  
403 compared to <sup>210</sup>Pb).  
404

405 Other advantages and disadvantages of  $^{137}\text{Cs}$  vs.  $^{210}\text{Pb}$  radioisotope dating are presented in Table 3.  $^{137}\text{Cs}$  deposition was a  
406 pulse that occurred in 1954 and 1963. At the 1963 peak, the activity ~~is declining~~declined with time because of two factors:  
407 (1) peak natural radioactive decay, with the  $^{137}\text{Cs}$  30-year half-life reducing the peak size over time, and (2) peak attenuation  
408 due to physical, chemical, or biological reasons (Drexler et al. 2018). The declining  $^{137}\text{Cs}$  activity limits its applicability as a  
409 radioisotope dating tool; however, recent studies have reported adequate  $^{137}\text{Cs}$  reference inventories for Canadian landscapes  
410 (Sutherland, 1991; Kachanoski and Von Bertoldi, 1996; Li et al., 2008; Mabit et al., 2014; Zarrinabadi et al., 2023). In  
411 addition, the use of  $^{137}\text{Cs}$  inventory for dating to complement the peak has addressed the potential inadequacies that could be  
412 attributed to declining peak resolution with ~~the passage of~~time.  $^{137}\text{Cs}$  dating is advantageous for its simplicity in pre- and  
413 post-processing of samples and the presence of additional time-markers in other regions (Breithaupt et al., 2018; Foucher et  
414 al., 2021). For example, ~~there are~~additional time-markers ~~corresponding~~correspond to the 1986 Chernobyl nuclear plant  
415 accident and 2011 Fukushima accident, ~~although~~. However, their effect ~~is less felt~~has yet to be recorded in North America  
416 due to the substantial distance from the source. Recognizing that there may be regional or local variation in peaks, we used  
417 non-eroded  $^{137}\text{Cs}$  reference sites to deal with regional variation in deposition. We also used multiple sampling sites within  
418 wetlands to assess local variation in deposition. Further, we looked for evidence from Chernobyl and Fukushima nuclear  
419 events in our data but found none (data not shown).

420  
421 Further, we looked for evidence from Chernobyl and Fukushima nuclear events in our data but found none (data not shown).  
422  $^{137}\text{Cs}$  dating is best suited for where the total OC is sequestered since a fixed time-marker (1954 onset or 1963 peak) or the  
423 average OC sequestration rate ~~over that period~~is needed. In contrast, the atmospheric deposition of  $^{210}\text{Pb}$  is continuous and,  
424 therefore, not limited in its applicability as a radioisotope dating tool.  $^{210}\text{Pb}$  dating is best suited for where variable OC  
425 sequestration rates are needed over a ~~longer~~more extended period (earlier than 1954).  $^{210}\text{Pb}$  dating is advantageous because  
426 its calculations are based on multiple points ~~and can provide several time markers~~associated with progressive OC  
427 sequestration rates derived using a constant rate of supply model—including the 1954 onset and 1963 peak of  $^{137}\text{Cs}$   
428 activity—improving the precision of the OC sequestration rates. This precision enables estimating OC sequestration rates  
429 when wetlands are not ~~intact~~undisturbed (history of drainage or at different ages since restoration) and ~~intact~~undisturbed (no  
430 history of drainage).

431  
432

**Table 3: Advantages** The advantages and disadvantages of using  $^{137}\text{Cs}$  and unsupported  $^{210}\text{Pb}$  ( $^{210}\text{Pb}_{\text{ex}}$ ) to estimate wetland organic carbon (OC) sequestration rates **in wetlands.**

Method of radiometric dating	$^{137}\text{Cs}$	$^{210}\text{Pb}_{\text{ex}}$
Advantages	<ul style="list-style-type: none"> <li>• Calculations are based on single points representing the peak (1963) and onset (1954) of the fallout. There are additional time-markers for Europe (1986 due to the Chernobyl nuclear accident) and Japan (2011 due to Fukushima Daiichi nuclear accident).</li> <li>• Sedimentation peak may still be evident allowing estimation of OC sequestration rate even if parts of the sediment core are disturbed.</li> <li>• Sedimentation rate can be estimated using gamma detection, which is non-destructive, so sample can be re-analyzed or used for other analyses.</li> <li>• Less sample preparation time for gamma analysis.</li> <li>• After the <math>^{137}\text{Cs}</math> activity is measured, post-processing of data is less challenging.</li> </ul>	<ul style="list-style-type: none"> <li>• Calculations are based on multiple points as there is continuous atmospheric deposition.</li> <li>• Sedimentation rate can be estimated using two reliable methods i.e., both alpha and gamma detection.</li> <li>• Less sample preparation time for gamma analysis compared to alpha.</li> <li>• Gamma analysis is non-destructive, so samples can be re-analyzed for other analyses compared to alpha.</li> <li>• Can run multiple samples at a time on a single detector in alpha method.</li> </ul>



Method of radiometric dating	$^{137}\text{Cs}$	$^{210}\text{Pb}_{\text{ex}}$
Disadvantages	<ul style="list-style-type: none"> <li>• Risk of mixing of restored and drained states when estimating OC sequestration rates due to specificity of the 1954 and 1963 time-markers (e.g., if drained and restored after 1963).</li> <li>• Declining atmospheric deposition and declining inventory due to radioactive decay (i.e., with no more nuclear testing, atmospheric deposition only comes from recent accidental releases from Chernobyl and Fukushima).</li> <li>• Sometimes the peak is not distinct.</li> <li>• Can be estimated using only one reliable method i.e., Gamma detection.</li> <li>• Can run only one sample at a time on a single detector.</li> <li>• Sensitive to vertical mobilization of sediments.</li> <li>• Sensitive to declining <math>^{137}\text{Cs}</math> inventory due to radioactive decay.</li> <li>• Sensitive to changes in redox potential.</li> <li>• More sensitive to biological and chemical activity compared to <math>^{210}\text{Pb}</math> (e.g., <math>^{137}\text{Cs}</math> can be taken up by plants instead of sodium or potassium, and <math>^{137}\text{Cs}</math> is soluble and therefore subject to mobility into solution then moving up and down the core).</li> </ul>	<ul style="list-style-type: none"> <li>• Requires full profile of <math>^{210}\text{Pb}</math> to do the calculations, if the sediment core disturbed then it cannot be used to estimate OC sequestration rates.</li> <li>• Sensitive to vertical mobilization of sediments, but not as much as <math>^{137}\text{Cs}</math>.</li> <li>• The alpha method is destructive, and therefore the sample is not available for re-use or re-analysis.</li> <li>• The alpha method requires extra precaution using hydrochloric acid for digesting, heating, spiking with <math>^{209}\text{Po}</math> tracer (i.e., analysts come in direct contact with radioactive material <math>^{209}\text{Po}</math> and hot acid).</li> <li>• The alpha method takes more time per sample (i.e., overnight digest followed by at least 48 h on the alpha counter), and is more labor intensive i.e., digest, engraving coins, plating, transferring into ensemble, etc.).</li> <li>• The alpha method requires more technical expertise for post processing of the data.</li> <li>• <a href="#">Uncertainty of <math>^{210}\text{Pb}_{\text{ex}}</math> results derived from gamma analysis can be higher than alpha.</a></li> </ul>

#### 434 4.1 Challenges in interpreting the $^{137}\text{Cs}$ peak

435 A potential weakness of  $^{137}\text{Cs}$  radioisotope dating arises from the challenges in interpreting the disturbed 1963 peak. The  
436 noise in the 1963 peak in wetlands on agricultural landscapes can be due to the redistribution of sediments since wetlands are  
437 susceptible to receiving a large mass of sediments resulting from various erosional processes due to their positioning within  
438 the landscape (Lobb et al., 2011; Zarrinabadi et al., 2023). Soil erosion resulting from wind, water, and/or tillage can lead to  
439 higher or lower  $^{137}\text{Cs}$  levels (Li et al., 2010; Foucher et al., 2021; Zarrinabadi et al., 2023) in wetlands in agricultural  
440 landscapes. If  $^{137}\text{Cs}$  enriched soil from the surrounding landscape gets deposited on top of the wetland's original soil layer ~~in~~  
441 ~~the wetland, then,~~ it can ~~lead to an increased~~ increase the  $^{137}\text{Cs}$  inventory value (Walling and Quine, 1991; Li et al., 2010).  
442 The magnitude of  $^{137}\text{Cs}$  enrichment depends on whether sediment comes from surface or sub-surface layers. (Li et al., 2010;  
443 Lal, 2020). For example, if the wetland receives  $^{137}\text{Cs}$  enriched topsoil post-1963 ~~then,~~ the  $^{137}\text{Cs}$  inventory would be higher  
444 than the  $^{137}\text{Cs}$  depleted subsoil.

445  
446 The screening of  $^{137}\text{Cs}$  profiles (Fig. ~~1a~~2a) considered the redistribution of sediments within the landscape ~~and~~. It  
447 demonstrated that the difficulty in disturbed  ~~$^{137}\text{Cs}$  profiles~~  $^{137}\text{C}$  profile interpretation can be reduced by investigating the  
448 cumulative  ~~$^{137}\text{Cs}$~~   $^{137}\text{C}$  inventory value. A cutoff cumulative  $^{137}\text{Cs}$  inventory value can ~~be useful in excluding~~ help exclude  
449 questionable profiles. The range of  $^{137}\text{Cs}$  reference inventory values from previous erosion studies within the study area (e.g.,  
450 Sutherland, 1991; Kachanoski and Von Bertoldi, 1996; Zarrinabadi et al., 2023) can help in establishing and setting the  
451 cutoff cumulative  $^{137}\text{Cs}$  inventory value. The mean  $^{137}\text{Cs}$  reference inventory values in the four provinces of Canada where  
452 our wetland sites are located ~~are~~ were utilized in this instance. The mean  $^{137}\text{Cs}$  reference inventory value estimated to be  
453 1,684 Bq m<sup>-2</sup> (coefficient of variation (CV) = 49%) for ~~AB,~~ three AB wetland sites (53° N and 113° W) (Zarrinabadi et al.  
454 2023), 989 Bq m<sup>-2</sup> (CV = 20%) for seven SK wetland sites (51° N and 107° W) (Sutherland, 1991), 1,008 Bq m<sup>-2</sup> (CV =  
455 ~~20.5%~~) for SK, 17.9%) for nine SK wetland sites (51° N and 104° W) (Sutherland, 1991), 1,430 Bq m<sup>-2</sup> (CV = 8.6%) for five  
456 MB, ~~and~~ wetland sites (50° N and 100° W) (Zarrinabadi et al. 2023), 1,273 Bq m<sup>-2</sup> (CV = ~~15~~8.8%) for three ON  
457 ~~(Sutherland, 1991,~~ wetland sites (43.3° N and 80.3° W) (Kachanoski and Von Bertoldi, 1996; ~~Zarrinabadi et al. 2023)~~ and  
458 1,534 Bq m<sup>-2</sup> (CV = 1.7%) for three ON wetland sites (45.6° N and 74.8° W) (Kachanoski and Von Bertoldi, 1996). The  
459  $^{137}\text{Cs}$  reference inventory values were decay-corrected to 2021 for comparability. The cutoff cumulative  $^{137}\text{Cs}$  inventory  
460 value for this study was selected by checking the minimum  $^{137}\text{Cs}$  reference inventory value of the local region, i.e., 546 Bq  
461 m<sup>-2</sup> (using values reported in Sutherland, 1991; Kachanoski and Von Bertoldi, 1996; Zarrinabadi et al. 2023). Hence, any  
462  $^{137}\text{Cs}$  inventory value less than 500 Bq m<sup>-2</sup> was considered questionable and ~~classified as~~ low-quality. Additionally, > 75% of  
463  $^{137}\text{C}$  profiles had a cumulative  $^{137}\text{Cs}$  inventory value of > 500 Bq m<sup>-2</sup>, indicating that ~~the~~ our wetland sites'  $^{137}\text{Cs}$  reference  
464 inventory value ~~for our wetland sites~~ is most likely around 500 Bq m<sup>-2</sup>.

465

466 ~~Variation~~Variations in both the  $^{137}\text{Cs}$  peak types (e.g., distinct, broadened, fluctuating, etc.) and in  $^{137}\text{Cs}$  inventory values in  
467 this study suggested that the  $^{137}\text{Cs}$  profiles were impacted by various regional erosional processes in the surrounding  
468 agricultural landscape. Recent evidence suggests that there may be an outward movement of sediment and  $^{137}\text{Cs}$  from the  
469 center of the wetlands to the riparian area (Zarrinabadi et al., 2023), suggesting that the base  $^{137}\text{Cs}$  inventory value observed  
470 in the center of wetlands from atmospheric deposition in the 1950s-1960s could be less than that of the non-eroded reference  
471  $^{137}\text{Cs}$  values from the surrounding catchment.  ~~$^{137}\text{Cs}$~~   $^{137}\text{C}$  inventory of a sediment core can further help ~~in the assignment~~  
472 ~~of assign~~ the  $^{137}\text{Cs}$  peak. For example, the  $^{137}\text{Cs}$  peak was repositioned in disturbed sediment cores with higher  $^{137}\text{Cs}$   
473 inventory, where the first discernable peak after the sharp rise from the onset of  $^{137}\text{Cs}$  activity and exceeding or around the  
474 reference value was assumed to be the original  $^{137}\text{Cs}$  peak.  $^{239+240}\text{Pu}$  isotopes, like  $^{137}\text{Cs}$ , are a product of nuclear testing and  
475 can be used to identify the peak of  $^{137}\text{Cs}$ . Future research will use  $^{239+240}\text{Pu}$  to replace  $^{137}\text{Cs}$  as  $^{137}\text{Cs}$  levels diminish.

## 476 4.2 Challenges in interpreting $^{137}\text{Cs}$ and $^{210}\text{Pb}$ profiles

477 Mobilization of  $^{137}\text{Cs}$  and  $^{210}\text{Pb}$  in the sediment often occurs in wetlands. Vertical mixing of  $^{137}\text{Cs}$  within sediments can be  
478 caused by remobilization and redistribution by wind and water, ice movement and inversion, disturbance by animals, and  
479 disturbance by humans that ditch and drain the wetlands; till through the wetland when it is dry; and let cattle access them for  
480 water which ~~cause~~causes disturbances to the bottom sediments (AndersonRobbins et al., 1987; Lobb et al., 19951977; Milan  
481 et al., 1995; JagereikovaTakahashi et al., 2015). Vertical mixing affects the profile by attenuating the peak upward and  
482 downward (which we addressed using the  $^{137}\text{Cs}$  inventory value and not just the peak when assessing the profile). Horizontal  
483 mixing of  $^{137}\text{Cs}$  dating within sediment occurs by physical movement of sediments into or out of the wetland, causing  
484 uneven distribution of the OC content, where accumulation may be high at the edges of open water of the wetland (Lobb et  
485 al., 2011; Zarrinabadi et al., 2023). This heterogeneity can be caused by ~~horizontal~~the horizontal focusing of sediments in  
486 sub-basins within a wetland, i.e., multiple center points. Sampling multiple sediment cores from individual wetlands can help  
487 capture the heterogeneity within the wetland. ~~If~~Suppose the  $^{137}\text{Cs}$  activity of most of the sediment cores from ~~an individual~~a  
488 particular wetland ~~are~~is noisy with a higher inventory value, ~~then~~ (e.g.,  $^{137}\text{Cs}$  profile of S-LO-I-W4-T2-CW-R2 in  
489 Supplementary Fig. 2a). In that case, the impact by erosional processes can be deduced with higher certainty ~~because the~~.  
490 The higher observed inventory value could ~~be a result of~~from the movement of enriched material via erosion/lateral flow to  
491 the center of the wetland, ~~therefore~~ increasing the ~~quantity~~number of  $^{137}\text{Cs}$  ~~from the value that would be expected if no new~~  
492 ~~enriched material was introduced via erosion/lateral flow~~. In this study, the assumption of no substantial downward mixing  
493 of  $^{137}\text{Cs}$  was supported by (1) sampling three cores from each wetland, (2) assessing the sharpness of the rise of the peaks (a  
494 sharp rise means negligible mixing), (3) examining the cumulative  $^{137}\text{Cs}$  inventory value and validating against the known  
495 reference level, (4) classifying  $^{137}\text{Cs}$  profiles, and (5) corroborating with  $^{210}\text{Pb}$  dating.

### 496 4.3 <sup>137</sup>Cs vs. <sup>210</sup>Pb derived OC sequestration rates and stocks

497 <sup>137</sup>Cs radioisotope dating using the 1954 or 1963 time-markers gives reasonable estimates of OC sequestration rates as  
498 compared to <sup>210</sup>Pb radioisotope dating. The <sup>137</sup>Cs-<sup>210</sup>Pb Q-Q plot of the 1963 OC sequestration rates is ~~in~~-closer ~~proximity~~  
499 ~~with~~to the 1:1-line, suggesting compatibility between <sup>137</sup>Cs- and <sup>210</sup>Pb-based estimates- (Fig. 5c and 5d). Conversely, the  
500 <sup>137</sup>Cs-<sup>210</sup>Pb Q-Q plot of the 1954 OC sequestration rates showed more deviation from the 1:1 line; <sup>137</sup>Cs-based OC  
501 sequestration rates were more dispersed and were higher than the <sup>210</sup>Pb-based OC sequestration rates- (Fig. 5a and 5b). The  
502 mean OC sequestration rates in Table 2 further verify the comparability of OC sequestration rates using the 1963 time-  
503 marker (mean <sup>137</sup>Cs OC sequestration rate is 0.63 Mg ha<sup>-1</sup> yr<sup>-1</sup> while mean <sup>210</sup>Pb OC sequestration rate is 0.68 Mg ha<sup>-1</sup> yr<sup>-1</sup>).  
504 The dispersion using the 1954 time-marker (mean <sup>137</sup>Cs OC sequestration rate is 1.02 Mg ha<sup>-1</sup> yr<sup>-1</sup> while mean <sup>210</sup>Pb OC  
505 sequestration rate is 0.67 Mg ha<sup>-1</sup> yr<sup>-1</sup>). Providing better sequestration rate estimates has consequences for estimating OC  
506 stocks with an improved degree of accuracy, which may provide policymakers with better tools to make informed carbon  
507 management decisions supported with data.

508  
509 To put our findings ~~in~~into practice and in the ~~wider~~broader OC sequestration perspective, we consider a scenario where two  
510 independent studies were performed using <sup>137</sup>Cs and <sup>210</sup>Pb (with the CFCS model) at the ~~same~~exact locations. If the cores  
511 were not selected based on the criteria we used to ~~select~~choose high-quality profiles, then these two studies' OC  
512 sequestration rate estimates are likely to disagree. However, we know and have demonstrated through our findings that they  
513 are linearly dependent, and the equation of our linear regression lines may be used to transform one estimate to the other.  
514 Consequently, if the cores were selected based on ~~the criteria of~~our selection ~~criteria~~, then one can expect the OC  
515 sequestration rate estimates to have similar values, which alleviates the interpretation challenges of having two different  
516 estimates from two independent studies. This observation may help with consistency when disagreements in estimates are  
517 observed. Another practical application of our findings may be in data augmentation. For example, if we have <sup>210</sup>Pb data for  
518 a set of locations and <sup>137</sup>Cs data for other locations, the linear regression equation could ~~be used to~~transform <sup>210</sup>Pb data to  
519 augment <sup>137</sup>Cs data, and vice versa. This can help data-driven modelling approaches ~~where~~, ~~whereas~~ larger datasets help ~~to~~  
520 achieve robust modelling tools. Similarly, because OC stocks can be derived from sequestration rates for specific years,  
521 estimates derived using one radioisotope can be used to estimate OC from a dataset derived from another estimate, further  
522 contributing to the augmentation of the corresponding OC stock data.

523  
524 Based on the results of this study, we recommend (1) using high-quality <sup>137</sup>Cs and <sup>210</sup>Pb profiles to estimate OC  
525 sequestration rates, (2) interpreting <sup>137</sup>Cs profiles from agricultural landscapes carefully from the perspective of  
526 redistribution of sediments, (3) using both <sup>137</sup>Cs and <sup>210</sup>Pb to compare and validate estimates if logistic approves. However,  
527 in case where one had to choose between <sup>137</sup>Cs and <sup>210</sup>Pb we recommend (1) For <sup>137</sup>Cs: use 1963 time-markers to estimate

528 OC sequestration rates (compared to 1954) since it is found to be most comparable with  $^{210}\text{Pb}$  dating techniques (CFCS  
529 model), (2) For  $^{210}\text{Pb}$  (CFCS model): OC sequestration rates from present to 1963 can be estimated with highest precision  
530 since we corroborated the estimates with  $^{137}\text{Cs}$ . However, we cannot comment on the precision of  $^{210}\text{Pb}$ -based OC  
531 sequestration rate estimation before 1963 based on the scope of this study.

## 532 **5 Conclusions**

533 Information regarding OC sequestration rates within ~~freshwater mineral soil wetlands~~ temperate inland wetland soils is  
534 crucial for evaluating the potential of these ecosystems to serve as natural climate solutions. Radiometric dating using  $^{137}\text{Cs}$   
535 and  $^{210}\text{Pb}$  presents a valuable tool for estimating the recent OC sequestration potential of wetlands. Notably, a robust 1:1  
536 linear correlation has been observed between  $^{137}\text{Cs}$ - and  $^{210}\text{Pb}$ -based OC sequestration rates in high-quality sediment profiles.

537  
538 While estimations based on the onset of  $^{137}\text{Cs}$  in 1954 or its peak in 1963 were reasonable, estimates anchored to the 1963  
539 peak of  $^{137}\text{Cs}$  exhibited closer alignment with those derived from  $^{210}\text{Pb}$  data (using the CFCS model). These findings suggest  
540 that estimates derived from ~~both~~  $^{137}\text{Cs}$  and  $^{210}\text{Pb}$  radioisotope dating methods are interchangeable and reasonably comparable  
541 when utilizing the 1963  $^{137}\text{Cs}$  time-marker.

542  
543 ~~The combined use of~~ Combining  $^{137}\text{Cs}$  and  $^{210}\text{Pb}$  tracers provides a comprehensive assessment of sedimentation rates. While  
544 one tracer offers an average ~~rate of~~ sedimentation rate over ~~a period exceeding~~ 60 years, the other provides a temporal trend  
545 over the same period. This interchangeability enables more thorough evaluations of the average sedimentation rate in  
546 wetlands, which is crucial for leveraging them as natural climate solutions.

547 **Code and data availability.** The R code for the distance sampling modelling along with the data to run the code is available  
548 at <https://doi.org/10.5281/zenodo.10951658>. The organic carbon (OC) sequestration rates data used to check the  
549 comparability of the radioisotope profiles can be found in the Supplement. The radioisotope profiles used for screening ~~can~~  
550 ~~be found~~ are in the paper and Supplement. ~~Other~~The paper and Supplement present other relevant data to support our  
551 conclusion ~~are presented in the paper and/or Supplement~~.

552  
553 **Author contributions.** The authors' contributions ~~of authors~~ are as follows: PM: methodology, field and lab analysis,  
554 statistical analysis and modelling, writing; IFC: conceptualization, methodology, field and lab analysis, editing, supervision;  
555 CGT: conceptualization, editing, supervision; EE: methodology, field and lab analysis, editing; and DAL: methodology, field  
556 and lab analysis, editing.

557  
558 **Competing interests.** The authors declare that they have no conflict of interest.

559  
560 **Acknowledgements.** We acknowledge the support of the Natural Sciences and Engineering Research Council of Canada  
561 (NSERC): Strategic Partnership Grant (STPGP 506809) to IFC, DAL, and CGT. Additional funding sources are the NSERC  
562 Canadian Graduate Scholarship, Saskatchewan Innovation and Opportunity Scholarship, PhD Scholarship, School of  
563 Environment and Sustainability, University of Saskatchewan, and Wanda Young Scholarship awarded to PM. We thank  
564 Jacqueline Serran, Kevin Erratt, Oscar Senar, Ehsan Zarrinabadi, and many others for assisting in field sampling.

565 **References**

- 566 ~~Anderson, R. F., Schiff, S. L., and Hesslein, R. H.: Determining sediment accumulation and mixing rates using  $^{210}\text{Pb}$ ,~~  
567  ~~$^{137}\text{Cs}$ , and other tracers: problems due to postdepositional mobility or coring artifacts, *Canadian Journal of*~~  
568 ~~*Fisheries and Aquatic Sciences*, 44(S1), s231-s250, doi:10.1139/f87-298, 1987.~~
- 569 Andersen, T. J., Mikkelsen, O. A., Møller, A. L., and Pejrup, M.: Deposition and mixing depths on some European intertidal  
570 mudflats based on  $^{210}\text{Pb}$  and  $^{137}\text{Cs}$  activities, *Continental Shelf Research*, 20(12-13), 1569-1591, doi:  
571 10.1016/S0278-4343(00)00038-8, 2000.
- 572 Appleby, P. G. and Oldfield, F.: The calculation of lead-210 dates assuming a constant rate of supply of unsupported  $^{210}\text{Pb}$   
573 to the sediment, *Catena*, 5(1), 1-8, doi:10.1016/S0341-8162(78)80002-2, 1978.
- 574 Appleby, P. G., and Oldfieldz, F.: The assessment of  $^{210}\text{Pb}$  data from sites with varying sediment accumulation rates,  
575 *Hydrobiologia*, 103, 29-35, doi:10.1007/BF00028424, 1983.
- 576 Bansal, S., Creed, I. F., Tangen, B. A., Bridgham, S. D., Desai, A. R., Krauss, K. W., Neubauer, S. C., Noe, G. B.,  
577 Rosenberry, D. O., Trettin, C., Wickland, K. P., Allen, S. T., Arias-Ortiz, A., Armitage, A. R., Baldocchi, D.,  
578 Banerjee, K., Bastviken, D., Berg, P., Bogard, M., Chow, A. T., Conner, W. H., Craft, C., Creamer, C., DelSontro,  
579 T., Duberstein, J. A., Eagle, M., Fennessy, M. S., Finkelstein, S. A., Göckede, M., Grunwald, S., Halabisky, M.,  
580 Herbert, E., Jahangir, M. M. R., Johnson, O. F., Jones, M. C., Kelleway, J. J., Knox, S., Kroeger, K. D., Kuehn, K.  
581 A., Lobb, D., Loder A. L., Ma, S., Maher, D. T., McNicol, G., Meier, J., Middleton, B. A., Mills, C., Mistry, P.,  
582 Mitra, A., Mobiiian, C., Nahlik, A. M., Newman, S., O'Connell, J. L., Oikawa, P., Post van der Burg, M., Schutte,  
583 C. A., Song, C., Stagg, C. L., Turner, J., Vargas, R., Waldrop, M. P., Wallin, M. B., Wang, Z. A., Ward, E. J.,  
584 Willard, D. A., Yarwood, S., and Zhu X.: Practical guide to measuring wetland carbon pools and  
585 fluxes, *Wetlands*, 43(8), 105, doi:10.1007/s13157-023-01722-2, 2023.
- 586 Bellucci, L. G., Frignani, M., Cochran, J. K., Albertazzi, S., Zaggia, L., Cecconi, G., and Hopkins, H.:  $^{210}\text{Pb}$  and  $^{137}\text{Cs}$  as  
587 chronometers for salt marsh accretion in the Venice Lagoon—links to flooding frequency and climate change,  
588 *Journal of Environmental Radioactivity*, 97(2-3), 85-102, doi:10.1016/j.jenvrad.2007.03.005, 2007.
- 589 Bernal, B. and Mitsch, W. J.: Comparing carbon sequestration in temperate freshwater wetland communities, *Global Change*  
590 *Biology*, 18(5), 1636-1647, doi:10.1111/j.1365-2486.2011.02619.x, 2012.
- 591 Bernal, B. and Mitsch, W. J.: Carbon sequestration in two created riverine wetlands in the Midwestern United States. *Journal*  
592 *of environmental quality*, 42(4), 1236-1244, doi:10.2134/jeq2012.0229, 2013.

- 593 Breithaupt, J. L., Smoak, J. M., Byrne, R. H., Waters, M. N., Moyer, R. P., and Sanders, C. J.: Avoiding timescale bias in  
594 assessments of coastal wetland vertical change, *Limnology and Oceanography*, 63(S1), S477-S495,  
595 doi:10.1002/lno.10783, 2018.
- 596 [Bridgham, S. D., Megonigal, J. P., Keller, J. K., Bliss, N. B., and Trettin, C.: The carbon balance of North American  
597 wetlands, \*Wetlands\*, 26\(4\), 889-916, doi:10.1672/0277-5212\(2006\)26\[889:TCBONA\]2.0.CO;2, 2006.](#)
- 598 Burnham K. P. and Anderson D. R. (Eds.): *Model Selection and Multimodel Inference: A Practical Information-Theoretic  
599 Approach*, Springer, doi:10.1007/b97636, 2003.
- 600 Craft, C. B. and Casey, W. P.: Sediment and nutrient accumulation in floodplain and depressional freshwater wetlands of  
601 Georgia, USA. *Wetlands*, 20(2), 323-332, doi:10.1672/0277-5212(2000)020[0323:SANAIF]2.0.CO;2, 2000.
- 602 Craft, C. B. and Richardson, C. J.: Recent and long-term organic soil accretion and nutrient accumulation in the  
603 Everglades, *Soil Science Society of America Journal*, 62(3), 834-843,  
604 doi:10.2136/sssaj1998.03615995006200030042x, 1998.
- 605 Craft, C., Vymazal, J., and Kröpfelová, L.: Carbon sequestration and nutrient accumulation in floodplain and depressional  
606 wetlands. *Ecological Engineering*, 114, 137-145, doi:10.1016/j.ecoleng.2017.06.034, 2018.
- 607 Creed, I. F., Badiou, P., Enanga, E., Lobb, D. A., Pattison-Williams, J. K., Lloyd-Smith, P., and Gloutney, M.: Can  
608 restoration of freshwater mineral soil wetlands deliver nature-based climate solutions to agricultural landscapes?,  
609 *Frontiers in Ecology and Evolution*, 10, 932415, doi:10.3389/fevo.2022.932415, 2022.
- 610 DeLaune, R. D., Jugsujinda, A., Peterson, G. W., and Patrick Jr, W. H.: Impact of Mississippi River freshwater  
611 reintroduction on enhancing marsh accretionary processes in a Louisiana estuary, *Estuarine, Coastal and Shelf  
612 Science*, 58(3), 653-662, doi:10.1016/S0272-7714(03)00177-X, 2003.
- 613 Drexler, J. Z., Fuller, C. C., and Archfield, S.: The approaching obsolescence of <sup>137</sup>Cs dating of wetland soils in North  
614 America, *Quaternary Science Reviews*, 199, 83-96, doi:10.1016/j.quascirev.2018.08.028, 2018.
- 615 [Environment and Climate Change Canada \(ECCC\): Canadian Environmental Sustainability Indicators: Extent of Canada's  
616 Wetlands, ECCC, Gatineau, Quebec, \[www.ec.gc.ca/indicateurs-indicators/default.asp?lang=en&n=69E2D25B-1\]\(http://www.ec.gc.ca/indicateurs-indicators/default.asp?lang=en&n=69E2D25B-1\),  
617 last access: 10 July 2024, 2016.](#)
- 618 Foucher, A., Chaboche, P. A., Sabatier, P., and Evrard, O.: A worldwide meta-analysis (1977–2020) of sediment core dating  
619 using fallout radionuclides including <sup>137</sup>Cs and <sup>210</sup>Pb xs, *Earth System Science Data Discussions*, 2021, 1-61,  
620 doi:10.5194/essd-13-4951-2021, 2021.
- 621 ~~Jagereikova, M., Cornu, S., Le Bas, C., and Evrard, O.: Vertical distributions of <sup>137</sup>Cs in soils: a meta-analysis, *Journal of  
622 Soils and Sediments*, 15, 81-95, doi:10.1007/s11368-014-0982-5, 2015.~~



- 623 Hambäck, P. A., Dawson, L., Geranmayeh, P., Jarsjö, J., Kačergytė, I., Peacock, M., Collentine, D., Destouni, G., Futter,  
624 M., Hugelius, G., Hedman, S., Jonsson, S., Klatt, B. K., Lindström, A., Nilsson, J. E., Pärt, T., Schneider, L. D.,  
625 Strand, J. A., Urrutia-Cordero, P., Åhlén, D., Åhlén, I., and Blicharska, M.: Tradeoffs and synergies in wetland  
626 multifunctionality: A scaling issue. *Science of the Total Environment*, 862, 160746,  
627 doi:10.1016/j.scitotenv.2022.160746, 2023.
- 628 Hoogsteen, M. J., Lantinga, E. A., Bakker, E. J., Groot, J. C., and Tittonell, P. A.: Estimating soil organic carbon through  
629 loss on ignition: effects of ignition conditions and structural water loss, *European Journal of soil science*, 66(2),  
630 320-328, doi:10.1111/ejss.12224, 2015.
- 631 Jain, J. L., Mohanty, S. G., and Böhm, W.: *A Course on Queueing Models*, Chapman and Hall/CRC, doi:10.1201/b15892,  
632 2007.
- 633 Kachanoski, R. G. and Von Bertoldi, P.: *Monitoring soil loss and redistribution using 137 Cs*, COESA Report No.  
634 RES/MON-008/96, Green Plan Research Sub-program, Agriculture and Agri-food Canada, London, Ontario, 1996.
- 635 Klaminder, J., Appleby, P., Crook, P., and Renberg, I.: Post-deposition diffusion of 137Cs in lake sediment: Implications for  
636 radiocaesium dating, *Sedimentology*, 59: 2259–2267, doi:10.1111/j.1365-3091.2012.01343.x, 2012.
- 637 Kamula, C. M., Kuzyk, Z. Z. A., Lobb, D. A., and Macdonald, R. W.: Sources and accumulation of sediment and particulate  
638 organic carbon in a subarctic fjord estuary: 210Pb, 137Cs, and  $\delta^{13}\text{C}$  records from Lake Melville,  
639 Labrador, *Canadian Journal of Earth Sciences*, 54(9), 993-1006, doi:10.1139/cjes-2016-0167, 2017.
- 640 Kolthoff, I. M. and Sandell, E. B.: *Textbook of quantitative inorganic analysis*, The Macmillan Company,  
641 doi:10.1002/sce.3730380480, 1952.
- 642 Lal, R. (2020). *Soil erosion and gaseous emissions*. *Applied Sciences*, 10, 2784, doi:10.3390/app10082784, 2020.
- 643 Li, S., Lobb, D. A., Lindstrom, M. J., and Farenhorst, A.: Tillage and water erosion on different landscapes in the northern  
644 North American Great Plains evaluated using 137Cs technique and soil erosion models, *Catena*, 70(3), 493-505,  
645 doi:10.1016/j.catena.2006.12.003, 2007.
- 646 Li, S., Lobb, D. A., Lindstrom, M. J., and Farenhorst, A.: Patterns of water and tillage erosion on topographically complex  
647 landscapes in the North American Great Plains, *journal of soil and water conservation*, 63(1), 37-46,  
648 doi:10.2489/jswc.63.1.37, 2008.
- 649 Li, S., Lobb, D. A., Tiessen, K. H., and McConkey, B. G.: Selecting and applying cesium-137 conversion models to estimate  
650 soil erosion rates in cultivated fields, *Journal of environmental quality*, 39(1), 204-219, 2010.  
651 doi:10.2134/jeq2009.0144, 2010.

- 652 Lobb, D. A.: Understanding and managing the causes of soil variability, *Journal of Soil and Water Conservation*, 66(6),  
653 175A-179A, doi:10.2489/jswc.66.6.175A, 2011.
- 654 ~~Lobb, D. A., Kachanoski, R. G., and Miller, M. H.: Tillage translocation and tillage erosion on shoulder slope landscape~~  
655 ~~positions measured using 137Cs as a plotter, *Canadian Journal of Soil Science*, 75 (2), 211-218, doi:10.4141/cjss95-~~  
656 ~~029, 1995.~~
- 657 Loder, A. L., and Finkelstein, S. A.: Carbon accumulation in freshwater marsh soils: A synthesis for temperate North  
658 America, *Wetlands*, 40(5), 1173-1187, doi:10.1007/s13157-019-01264-6, 2020.
- 659 Mabit L., Kieth, S. C., Dornhofer, P., Toloza, A., Benmansour, M., Bernard, C., Fulajtar, E., and Walling D. E.: 137Cs: A  
660 widely used and validated medium term soil tracer, *Guidelines for Using Fallout Radionuclides to Assess Erosion*  
661 *and Effectiveness of Soil Conservation Strategies*, IAEA-TECDOC-1741, Vienna, doi:10.13140/2.1.2586.1122,  
662 2014.
- 663 Milan, C. S., Swenson, E. M., Turner, R. E., and Lee, J. M.: Assessment of the method for estimating sediment accumulation  
664 rates: Louisiana salt marshes, *Journal of Coastal Research*, 296-307, <https://www.jstor.org/stable/4298341>, 1995.
- 665 Miller, D. L. and Clark-Wolfe, T. J.: Package “Distance”, <https://cran.r-project.org/web/packages/Distance/Distance.pdf>,  
666 2023.
- 667 Miller, D. L., Rexstad, E., Thomas, L., Marshall, L., and Laake, J. L.: Distance sampling in R. *Journal of Statistical*  
668 *Software*, 89(1), 1–28, doi:10.18637/jss.v089.i01, 2019.
- 669 Nahlik, A. M. and Fennessy, M. S.: Carbon storage in US wetlands. *Nature Communications*, 7(1), 1-9,  
670 doi:10.1038/ncomms13835, 2016.
- 671 Owens, P. N. and Walling, D. E.: Spatial variability of caesium-137 inventories at reference sites: an example from two  
672 contrasting sites in England and Zimbabwe, *Applied Radiation and Isotopes*, 47(7), 699-707, doi:10.1016/0969-  
673 8043(96)00015-2, 1996.
- 674 Pennington, W., Tutin, T. G., Cambray, R. S., and Fisher, E. M.: Observations on lake sediments using fallout 137Cs as a  
675 tracer, *Nature*, 242(5396), 324-326, doi:10.1038/242324a0, 1973.
- 676 Pribyl, D. W.: A critical review of the conventional SOC to SOM conversion factor, *Geoderma*, 156(3-4), 75-83,  
677 doi:10.1016/j.geoderma.2010.02.003, 2010.
- 678 R Core Team: R: A language and environment for statistical computing, R Foundation for Statistical Computing, Vienna,  
679 Austria, <https://www.R-project.org/>, 2023.

- 680 Ritchie, J. C. and McHenry, J. R.: Application of radioactive fallout cesium-137 for measuring soil erosion and sediment  
681 accumulation rates and patterns: A review. *Journal of environmental quality*, 19(2), 215-233,  
682 doi:10.2134/jeq1990.00472425001900020006x, 1990.
- 683 Robbins, J.A., Krezoski, J.R. and Mozley, S.C.: Radioactivity in sediments of the Great Lakes: post-depositional  
684 redistribution by deposit-feeding organisms, *Earth Planet. Sci. Lett.*, 36, 325–333, doi: 10.1016/0012-  
685 821X(77)90217-5, 1977.
- 686 Sanchez-Cabeza, J. A. and Ruiz-Fernández, A. C.: 210Pb sediment radiochronology: an integrated formulation and  
687 classification of dating models, *Geochimica et Cosmochimica Acta*, 82, 183-200, doi:10.1016/j.gca.2010.12.024,  
688 2012.
- 689 Sutherland, R. A.: Examination of caesium-137 areal activities in control (uneroded) locations, *Soil technology*, 4(1), 33-50,  
690 doi:10.1016/0933-3630(91)90038-O, 1991.
- 691 Takahashi, J., Tamura, K., Suda, T., Matsumura, R., and Onda, Y.: Vertical distribution and temporal changes of 137Cs in  
692 soil profiles under various land uses after the Fukushima Dai-ichi Nuclear Power Plant accident, *Journal of*  
693 *environmental radioactivity*, 139, 351-361, doi:10.1016/j.jenvrad.2014.07.004, 2015.
- 694 United Nations Scientific Committee on the Effects of Atomic Radiation (UNSCEAR): Sources and Effects of Ionizing  
695 Radiation, V1, United Nations, New York, doi:10.18356/49c437f9-en, 2000.
- 696 Villa, J. A. and Bernal, B.: Carbon sequestration in wetlands, from science to practice: An overview of the biogeochemical  
697 process, measurement methods, and policy framework, *Ecological Engineering*, 114, 115-128,  
698 doi:10.1016/j.ecoleng.2017.06.037, 2018.
- 699 Walling, D. E. and He, Q.: Using fallout lead-210 measurements to estimate soil erosion on cultivated land. *Soil Science*  
700 *Society of America Journal*, 63(5), 1404-1412, doi:10.2136/sssaj1999.6351404x, 1999.
- 701 Walling, D. E. and Quine, T. A.: Use of 137Cs measurements to investigate soil erosion on arable fields in the UK: potential  
702 applications and limitations, *Journal of Soil Science*, 42(1), 147-165, doi:10.1111/j.1365-2389.1991.tb00099.x,  
703 1991.
- 704 Zaborska, A., Carroll, J., Papucci, C., and Pempkowiak, J.: Intercomparison of alpha and gamma spectrometry techniques  
705 used in 210Pb geochronology. *Journal of environmental radioactivity*, 93(1), 38-50,  
706 doi:10.1016/j.jenvrad.2006.11.007, 2007.
- 707 Zarrinabadi, E., Lobb, D. A., Enanga, E., Badiou, P., and Creed, I. F.: Agricultural activities lead to sediment infilling of  
708 wetlandscapes in the Canadian Prairies: Assessment of soil erosion and sedimentation fluxes, *Geoderma*, 436,  
709 116525, doi:10.1016/j.geoderma.2023.116525, 2023.

710 Zhang, F., Wang, J., Baskaran, M., Zhong, Q., Wang, Y., Paatero, J., and Du, J.: A global dataset of atmospheric  $^7\text{Be}$  and  
711  $^{210}\text{Pb}$  measurements: annual air concentration and depositional flux, *Earth System Science Data*, 13(6), 2963-  
712 2994, doi:10.5194/essd-13-2963-2021, 2021.